Maria Beatriz Ribeiro Felgueiras

Licenciatura em Ciências Biomédicas

Investigating chitotriosidase and glycosyltransferase GLT8D1 in Amyotrophic Lateral Sclerosis

Dissertação para obtenção do Grau de Mestre em
Bioquímica para a Saúde

Orientador: Prof. Dr. Júlia Costa, Principal Investigador, ITQB

Novembro, 2021

Maria Beatriz Ribeiro Felgueiras

Licenciatura em Ciências Biomédicas

Investigating chitotriosidase and glycosyltransferase GLT8D1 in Amyotrophic Lateral Sclerosis

Dissertação para obtenção do Grau de Mestre em
Bioquímica para a Saúde

Orientador: Prof. Dr. Júlia Costa, Principal Investigador, ITQB

Júri:

Presidente: Prof. Doutor Pedro Manuel Henriques Marques Matias
Arguente: Prof. Doutora Marta Luísa Gromicho Morgado da Silva
Vogais: Prof. Doutora Júlia Carvalho Costa
Prof. Doutora Ana Maria de Jesus Bispo Varela Coelho

Instituto de Tecnologia Química e Biológica

Novembro, 2021

Copyright

Acknowledgments

The big accomplishments in life can never be achieve without help and support, and so I would like to express my gratitude to the people who helped me throughout this journey.

Firstly, I would like to express my best gratitude to Dr. Júlia Costa my supervisor, for the opportunity, the persistency, the guidance, and for being the most important factor in my growth in the investigation world.

To Prof. Dr. Mamede de Carvalho (Hospital de Santa Maria, Faculdade de Medicina de Lisboa) for the plasma samples that were used in this study, plus the demographic and clinical parameters of the patients. To Dr. Abel Oliva for the training to use the ELISA plate reader (ITQB NOVA). To Dr. Cristina Peixoto for allowing me to use the plate reader for enzymatic activity assays, and for all the help offered by the laboratory group members (iBET). To Conceição Almeida, Catarina Correia, Dr. Ana Guerreiro (UniMS, ITQB NOVA, iBET) for the acquisition and interpretations of UHPLC-MS/MS data. To Dr. Pedro Lamosa for the acquisition of NMR results (CERMAX, ITQB NOVA). To Prof. K. Moremen (Complex Carbohydrate Research Center, University of Georgia, Athens, USA) for the gift of purified sGLT8D1. To Prof. P. Shaw and Prof J. Cooper-Knock (Sheffield Institute for Translational Neuroscience, SITraN, University of Sheffield, UK) for the gift of cells overexpressing GLT8D1-wt and GLT8D1-R92C.

A special thanks goes to my friends Rafaela and Rebeca for during this year take my mind out of stress, being my support system and still taking me to eat in some of the best places ever, nothing but love for you guys.

Ao meu irmão, que mostra o que é ser um irmão mais velho, que me apoia, ajuda e está lá quando preciso e até quando não sei que preciso, sempre foste o meu modelo a seguir e sempre serás.

Por fim, mas mais importante, aos meus pais, Anselmo e Lurdes, a quem sem dúvida dedico este trabalho. Obrigada por serem quem são, por me apoiarem, por não me deixarem desistir daquilo que consigo ser e pelo amor incondicional que sempre tive de vocês.

Abstract

Amyotrophic lateral sclerosis (ALS) is a neurodegenerative neuromuscular disease causing motor neuron dysfunction. The identification of ALS biomarkers is of great importance in diagnosis, monitoring of disease progression and understanding of disease etiology.

The aim of this thesis was to investigate two proteins related with ALS pathology. First, the potential of plasma chitotriosidase (CHIT1) as ALS biomarker has been investigated. Second, the enzyme glycosyltransferase 8 domain-containing protein 1 (GLT8D1), recently found mutated in familial cases of ALS, has been characterized.

For CHIT1 quantification an enzyme-linked immunosorbent assay (ELISA) has been developed. Then, CHIT1 has been quantified from the plasma of 40 ALS patients and 11 healthy controls. The results showed a trend towards an increase in plasma CHIT1 levels for ALS patients (33621 pg/mL) comparatively to controls (20017 pg/mL) but the difference was not significant ($p = 0.083$). There was no correlation found with any of the scored demographic and clinical parameters, including disease progression or forced vital capacity (FVC).

Full-length membrane bound GLT8D1-wild type was compared with the ALS mutant GLT8D1-R92C. Results showed the mutation did not cause dimerization of the protein. Digestion with peptide N-glycosidase F and endoglycosidase H showed that both forms were N-glycosylated with high mannose/hybrid glycans. Distinctively, a soluble secretory form of the protein (sGLT8D1) was found to be N-glycosylated with high mannose/hybrid and complex glycans.

Towards elucidation of the specificity of sGLT8D1, a panel of acceptor substrates has been explored using UDP-galactose as nucleotide sugar donor. GLT8D1 was confirmed as a galactosyltransferase and N-acetylglucosamine was found to be an acceptor of the enzyme.

In conclusion, this work showed that CHIT1 from plasma did not have promising potential as ALS biomarker. Concerning GLT8D1 the results opened novel perspectives to explore endogenous cellular substrates of the enzyme aiming at elucidating its function and implications in disease.

Keywords- Amyotrophic Lateral Sclerosis, biomarker, plasma, chitotriosidase, glycosyltransferase 8 domain-containing 1, galactosyltransferase

Resumo

A esclerose lateral amiotrófica (ELA) é uma doença neuromuscular neurodegenerativa que causa disfunção dos neurónios motores. A identificação de biomarcadores é muito importante em diagnóstico, para monitorizar a progressão e compreender a etiologia da doença.

O objetivo desta tese foi investigar duas proteínas relacionadas com a patologia de ELA. Primeiro, foi investigado o potencial da quitotriosidase (CHIT1) do plasma como biomarcador para ELA. Em seguida, caracterizou-se a *glycosyltransferase 8 domain-containing protein 1* (GLT8D1), recentemente encontrada mutada em casos familiares de ELA.

Para a quantificação de CHIT1 foi desenvolvido um ensaio de ELISA o qual foi utilizado para quantificar CHIT1 no plasma de 40 pacientes com ELA e 11 controlos saudáveis. Os resultados mostraram um aumento dos níveis de CHIT1 no plasma nos pacientes (33621 pg/mL) comparativamente aos controlos (20017 pg/mL), mas a diferença não foi significativa ($p = 0.083$). Não foi encontrada correlação com nenhum dos parâmetros demográficos e clínicos registados, incluindo progressão da doença e capacidade vital forçada.

A proteína nativa de membrana GLT8D1 foi comparada com o mutante ELA GLT8D1-R92C. Os resultados mostraram que a mutação não provocava dimerização da proteína. A digestão com péptido N-glicosidase F e endoglicosidase H mostrou que ambas as formas eram N-glicosiladas com glicanos oligomanosídicos/híbridos. Por outro lado, uma forma solúvel secretada da proteína (sGLT8D1) era N-glicosilada com glicanos oligomanosídicos/híbridos e complexos.

Para elucidação da especificidade do substrato da sGLT8D1, foi explorado um painel de substratos aceitadores utilizando UDP-galactose como dador de açúcar nucleótido. GLT8D1 foi confirmada como galactosiltransferase e identificou-se a N-acetilglucosamina como aceitador da enzima.

Em conclusão, este trabalho mostrou que a CHIT1 do plasma não constituía um biomarcador promissor de ELA. No que diz respeito à GLT8D1, os resultados abriram novas perspetivas para explorar substratos celulares endógenos da enzima com vista à elucidação da sua função e implicações em doença.

Palavras-chave- Esclerose Lateral Amiotrófica, biomarcador, plasma, quitotriosidase, *glycosyltransferase 8 domain-containing protein 1*, galactosiltransferase

Index

Index of figures

Index of tables and appendices

Abbreviations

ALS– Amyotrophic Lateral Sclerosis
ALSFRS– Amyotrophic Lateral Sclerosis Functional Rating Scale
ALSFRS-R– Amyotrophic Lateral Sclerosis Functional Rating Scale Revised
C/CPLs– Chitinase-like Proteins
CHIT1– Chitotriosidase
CNS– Central Nervous System
CSF– Cerebrospinal Fluid
EDTA– Ethylenediamine Tetraacetic acid
ELISA– Enzyme-linked immunosorbent assay
Endo-H– Endoglycosidase H
ER– Endoplasmic Reticulum
FALS– Familiar Amyotrophic Lateral Sclerosis
FTD– Frontotemporal Dementia
Glc– Glucose
Gal– Galactose
GalNAc– N-Acetylgalactosamine
GlcNAc– N-Acetylglucosamine
GLT1– Glial Glutamate Transporter 1
GLT8D1– Glycosyltransferase 8 domain-containing protein 1
HRP– Horseradish Peroxidase
Lac– Lactose
LacNAc– N-acetyllactosamine
LMN– Lower Motor Neuron
MW– Molecular Weight
NfH– Neurofilaments Heavy Chain
NfL– Neurofilaments Light Chain
PBS– Phosphate-Buffered Saline
PNGase F– Peptide N-glycosidase F
SALS– Sporadic Amyotrophic Lateral Sclerosis
SOD1– Superoxide dismutase 1
TBS– Tris-Buffered Saline
TCA– Trichloroacetic Acid
TDP-43– TAR DNA binding protein 43
TBS– Tris-Buffered Saline t
TTBS– Tris-Buffered Saline with 0.1% (w/v) Tween-20
UDP– Uridine Diphosphate
UMN– Upper Motor Neuron

1. Introduction

1.1. ALS history

Jean-Martin Charcot was the first to associate the link between the pathology of the anterior horn cells or motor neurons of the cranial nerves, observed only by autopsy, and the signs of clinical amyotrophy in patients. Charcot remarkably gave a complete and detailed description of this new clinical condition, using the denomination "amyotrophic lateral sclerosis" (ALS) for the first time in 1874. His description is still used with little to no differences in the present [1].

A conference hosted in Spain in 1990 arose with the goal of creating a diagnostic criteria that could be globally accepted, practical and that offered a process to improve clinical studies, therapeutic trials and molecular genetic research studies in ALS. From that conference, the El Escorial Criteria were created for the diagnosis of ALS in 1994 [2] and then revised in 2000 [3].
In 1993, *superoxide dismutase 1 (SOD1)* was the first causative gene recognized in ALS [4]. The SOD1-G93A transgenic mouse model was the first ALS model to emerge and is still used extensively in today's studies to better understand and discover its mechanisms. In December 1995, the FDA endorsed riluzole as the first ever drug to be used as a treatment for ALS, working as a sodium channel blocker and indirect glutamate antagonist [5].

While that part of the pharmacology evolved, an *"assessment of activities of daily living in patients with amyotrophic lateral sclerosis"* was published in 1996 [6] called amyotrophic lateral sclerosis functional rating scale (ALSFRS), being used to monitor the patient's progression of disability. A revised version, which incorporated further assessments along with the need for ventilatory support, was later created, the revised ALSFRS (ALSFRS-R) [7]. Edaravone (MCI-186), providing a modest slowing of functional decline in a selected cohort [8], was officially approved by the FDA in 2017 for the treatment of ALS. Unfortunately, it remains without the approval of the European Medicines Agency.

1.2. Epidemiology

Amyotrophic lateral sclerosis is fairly rare around the world, having an estimated incidence (number of new cases per year) of 1.75-3 cases per 100 000 people each year and a prevalence (total number of disease cases) of 10-12 cases per 100 000 in Europe [9].

Curiously, ALS risk is different across continents and ethnicities. For example, there are some immensely studied geographic regions, that have a higher prevalence in ALS cases, being of familiar cause [10]. ALS is an age-associated disease in most cases, and so, the average age at onset is between 58-63 years when talking about SALS and 40-60 years for FALS. The disease

rarely occurs before 35 years of age [11]. The survival rate can be extremely variable but overall, it is relatively short, lasting an average of three and a half years after onset [12].

1.3. Clinical features of ALS

ALS is a disease with a vast range of clinical features, meaning it possesses an enormous heterogeneity, making it extremely challenging to have a diagnosis and treatment. The spread and progression of ALS is typically distinct from patient to patient, due to its heterogeneousness, forcing the research for treatment to be individual. The most notorious characteristic is the coexistence of upper and lower motor neuron symptoms (UMN and LMN respectively) [13] showed in Figure 1.1.

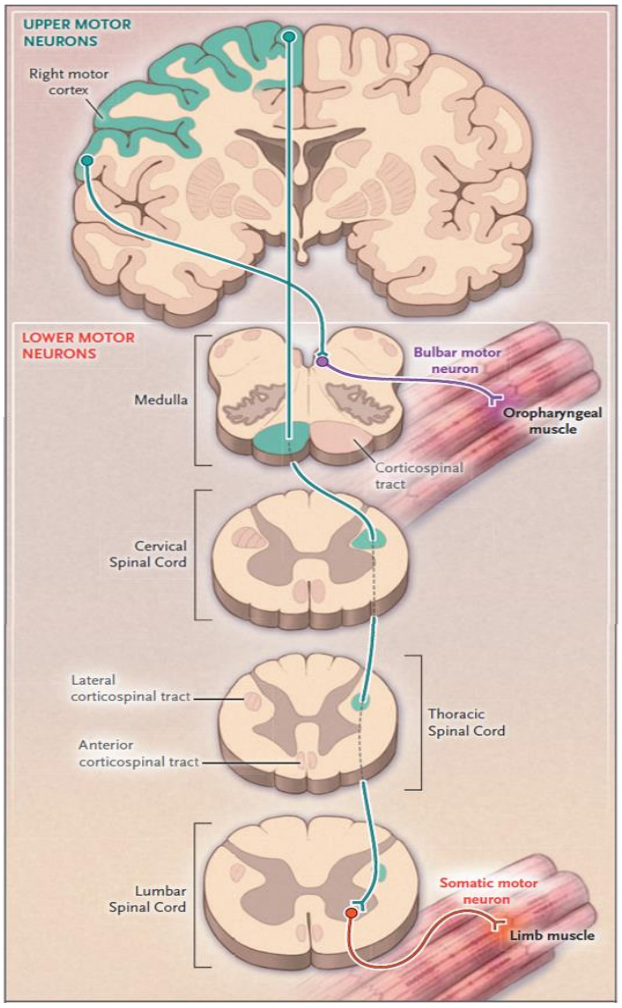

Figure 1.1- Motor Pathways. The motor system includes upper motor neurons (corticospinal) and the lower upper neurons (bulbar and spinal motor neurons). Figure adapted from [13].

There is evidence of hyperreflexia and spasticity in UMN and muscle atrophy and fasciculations in LMN, with manifestation of weakness in both. The affected motor neurons give rise to distinct clinical representations, defining the pattern of the symptoms. The

pathology major presentations are: limb onset (LO) with combinations of UMN and LMN involvement, bulbar onset (BO) having UMN and LMN present, primary lateral sclerosis (PLS) with only UMN involvement, and progressive muscular atrophy (PMA) with LMN involvement. Altogether, the clinical progress of those presentations provide the complete spectrum of ALS.

The main showcase of ALS is motor neuron dysfunction, which begins in one of the limbs or one region of the spinal cord and is classified as the LO. Initially it propagates locally, and the first symptoms occur in 70% of patients at the upper or lower limbs [14]. Roughly 20-25% of the cases initially arise in the cranial nerve nuclei, and in the bulbar muscles (oral, pharyngeal, and at times, respiratory muscles), and are called BO. Unfortunately, this percentage of patients tend to have a lower survival span, due to the important functions that the bulbar muscle possesses [15].

In patients presenting PLS there is a gradual progression of acute muscle spasticity and stiffness, with some muscle atrophy. Patients do not realize the presence of spasticity right away, they only notice it when it has an influence on their locomotor function, making them lose their balance and eventually fall [16]. The cognitive abilities are intact in ALS but around 5 to 10% of patients demonstrate an additional symptom which is dementia, mostly of the frontotemporal side of the brain (FTD) representing the harsh end of ALS spectrum. ALS/FTD has a tendency to be associated with BO ALS, establishing the most severe form of the disease, where motor signs and neuropsychological manifestations appear [17]. PMA is primarily presented with pure LMN involvement, and it may have either a slow or rapid progression, with severe arm/hand paralysis early into the development [18].

Although it starts in a particular location, the disease eventually will spread throughout the entire body. It extends to in-between neuroanatomically linked regions, and finally stopping muscle movement essential to survival [12].

1.4. Genetics of ALS

ALS can have two main triggers, the genetic origin representing approximately 5-10% of the cases, having the name of familiar ALS (FALS), or 90-95% sporadic origin (SALS) that arises without any prior familiar background [19].

In FALS the disease is genetically transmitted through primarily autosomal dominant mutations in certain genes, some which are represented in Table 1.1. Mutations in particular genes directly cause motor neuron degeneration and disease onset. Even though FALS cases represent a small percentage of ALS cases, the study and identification of genes involved is of extreme relevance. Through such genes it is possible to develop *in vitro* and *in vivo*

experimental models in the laboratory, making it possible to study clinical symptoms and molecular mechanisms associated with the disease.

Table 1.1- Selected ALS associated genes

Locus	Gene	Protein	Onset	Mutation	Function	Discovery	Reference
21q22.11	*SOD1*	Cu/Zn superoxide dismutase 1	Adult	Autosomal dominant and recessive	Catalyzes superoxide radicals	1993	[20]
2q33.2	*ALS2*	Alsin	Juvenile	Autosomal recessive	Guanine-nucleotide releasing factor	2001	[21]
1p36.22	*TARDBP*	TAR DNA binding protein 43 (TDP-43)	Adult	Autosomal dominant	RNA binding protein	2008	[22]
10p13	*OPTN*	Optineurin	Adult	Unknown	Autophagy adaptor	2010	[23]
Xp11.21	*UBQLN2*	Ubiquilin 2	Adult/Juvenile	X-linked dominant	Autophagy adaptor	2011	[24]
9p21.2	*C9orf72*	c9RAN proteins	Adult	Autosomal dominant	Possible guanine nucleotide exchange factor	2011	[25]
16p11.2	*FUS/TLS*	Fused sarcoma	Adult	Unknown	RNA binding protein	2015	[26]
12q14.1	*TBK1*	Serine/threonine-protein kinase TBK	Adult	Autosomal dominant	Regulates autophagy and inflammation	2015	[27]
12q13.3	*KIF5A*	Kinesin Family Member 5A	Adult	Autosomal dominant	Cellular transport	2017	[28]
P362L	*TIA1*	TIA1 cytotoxic granule associated RNA binding protein	Adult	Unknown	Stress granule assembly	2017	[29]
p.D40G	*ANXA11*	Annexin A11	Adult	Autosomal dominant	Phospholipid and calcium-binding	2017	[30]
p.R92C	*GLT8D1*	Glycosyltransferase 8 domain-containing protein 1	Adult	Autosomal dominant	Unknown	2019	[31]

The remaining cases are of sporadic origin, and constitute the great majority of ALS cases, where the cause for the appearance of disease still remains unknown, even though there is the presence of mutations also found in FALS. It is believed that genes and environment interact with one another resulting in disease onset in some individuals [32]. Several neurodegenerative diseases are deemed to be the result of gene interactions, ageing (that is associated with cell damage), environmental risk conditions and a random risk factor, that only a small number of people have [33].

These dual forms of ALS do not differ from each other phenotypically, however several mutations have similar clinical phenotypes hinting that several mechanisms may be the cause for the disease development.

1.4.1. GLT8D1

Amongst the previously referred ALS-associated gene mutations, rising interest has been focused on a heterozygous p.R92C mutation within exon 4 of the gene encoding Glycosyltransferase 8 domain-containing protein 1 (GLT8D1) [31]. This mutation was identified in ALS through exome sequencing in autosomal dominant familial ALS cases. The protein's wild type and mutant forms have been localized and expressed within the Golgi apparatus as a transmembrane protein (Figure 1.2A) [31].

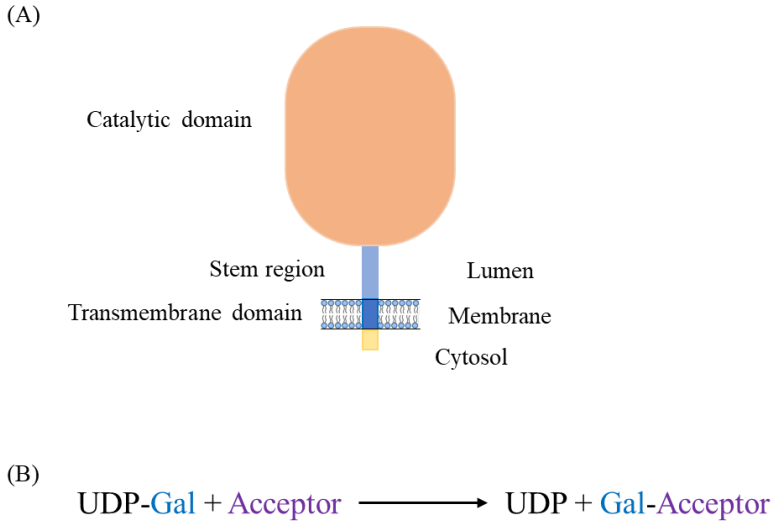

Figure 1.2- (A) Domain organization of a typical Golgi transmembrane glycosyltransferase **(B)** Possible schematic representation of enzymatic reaction of GLT8D1 catalyzing the transfer of a galactose from a donor molecule (UDP-Gal) to an acceptor.

In addition, the previously mentioned report showed that knockdown and overexpression of mutant GLT8D1 induced both motor neuron dysfunction and motor deficits in zebrafish embryos, which leads to consider the protein's role in neuron degeneration. Therefore, authors suggest that pathogenic *GLT8D1* mutations are associated with haploinsufficiency and/or a dominant-negative effect [31]. In other studies, genetic variants in this gene demonstrated a substantial increase in disease severity and cytotoxicity in ALS patients [34].

This class of proteins was not previously associated with neurodegeneration, although GLT8D1 has been identified as a risk gene in several other diseases such as schizophrenia. It is known that ALS and schizophrenia share common genetic risks, including gene *GLT8D1*, hitting an etiological relationship between the pathologies [35]. In addition, findings showed high rates of schizophrenia in relatives of patients with ALS [36]. GLT8D1 overexpression is also present in human cutaneous melanoma samples [37]. More recently, *GLT8D1* was also proven to be one of the risk genes that partially underlies the common genetic architecture of multiple psychiatric disorders such as bipolar disorder, autism spectrum disorder, attention deficit hyperactivity disorder and depression [38].

It is known that GLT8D1 has three N-glycosylation sites, and that such oligosaccharides are most likely involved in the initiation of the correct folding of some polypeptides in the ER and also participate in a quality control system [39]. Interest has been rising in protein glycosylation since it is a major post-translational modification and has been relevant in neurodegenerative diseases [40,41]. In addition, previous findings report that human glycosyltransferases are N-glycosylated [42].

GLT8D1 encodes a glycosyltransferase enzyme of unknown function. The involvement of glycosyltransferases has recently been investigated in the pathogenesis of neurodegenerative diseases [43–45]. The protein is a member of sugar nucleotide donor family 8 and it is expected to catalyze the transfer of a glycosyl group from a sugar nucleotide donor to an acceptor molecule [31,46]. In particular it is able to accept UDP-galactose as a donor (Figure 1.2B). Mutations are clustered close to the substrate binding domain in exon 4, reducing the enzyme's activity commensurate with an increase in substrate affinity, which is predicted to impair cycling of substrate through the enzyme, therefore, reducing overall GLT8D1 activity [31].

Interestingly, a recent study revealed that different ethnic backgrounds may influence *GLT8D1* as a risk gene for ALS and the subsequent mutations that impair its enzymatic activity, since no associations between the protein and the pathology were found in other populations [47].

More studies are needed to explore the enzyme's glycosylation and function in the cell. Additionally, crucial studies regarding the remaining components of this enzymatic activity, such as the specific acceptor molecule *in vivo*, and the formed bond between molecules, are yet to be determined in both wild type and mutant proteins.

Overall, far more investigation is required to improve our knowledge on the protein GLT8D1 regarding its structure and function in the organism.

1.5. Diagnostic

ALS has no clear and immediate diagnosis due to the broad array of clinical features, and so the diagnosis is mainly based on the identification of neuron lesions, associated with atrophy and loss of strength in several muscles.

The El Escorial criteria are practical criteria that offer a method to improve clinical studies, therapeutic trials and molecular genetic research studies aimed at ALS. The criteria are based on the identification of clinical signs of lesion of the motor neurons, lower or upper, combined with the absence of electrophysiological and neuroimaging evidence for other diseases that could explain the observed symptoms [2]. Some clinical neurophysiologists were concerned, claiming the sensitivity of the criteria was compromised, and so, the Awaji Criteria were created [48].

The most important exam patients must do is an electromyography (EMG) since it removes the possibility of any other disease involvement in the symptoms and also shows alterations in certain regions in the patient's body that are still clinically preserved.

ALSFRS is an approved scale based on questions, that measures the physical function in performing activities in the daily life of patients with the pathology. This measurement included evaluation of several aspects such as speech, swallowing, walking, amongst others [6], with a scale from 0 to 40. This scale was then revised and given the name ALSFRS-R [7]. This quiz has a score from 0 to 48, from worst disease condition to best, respectively therefore, making it possible to monitor progress of disease.

1.6. Mechanisms

Studies of tissue samples belonging to patients with ALS made it possible to observe the deterioration of the motor neurons. The deterioration was mainly located in the brain, more precisely in the motor cortex, in the brainstem motor nuclei and in the anterior horns of the spinal cord [49]. ALS pathogenic mechanisms that generate motor neuron degeneration are still being investigated, some of which are shown in Figure 1.3.

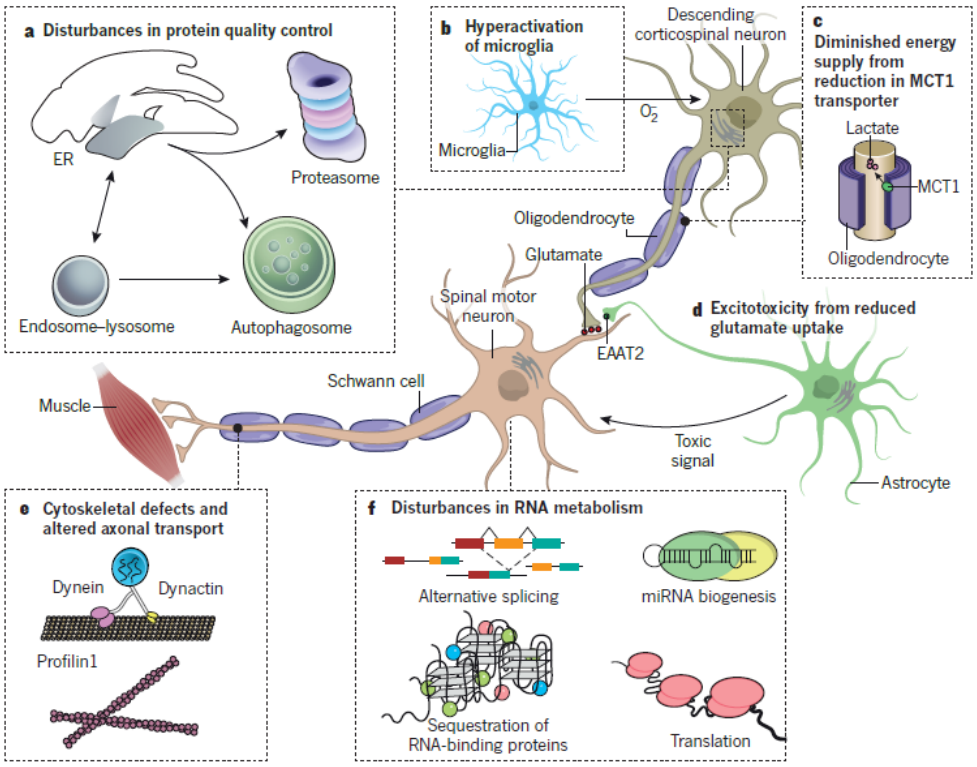

Figure 1.3- Pathological Mechanisms in ALS. a. Protein mutations affect elements involved in protein quality control; **b.** Microglia hyperactivation results in oxidative stress and neuroinflammation; **c.** Low levels of lactate transporter MCT1 provide low supplied energy from oligodendrocytes to motor neurons**; d.** Deficiency in the glutamate transporter EAAT2 results in excitotoxicity**; e.** Impaired axonal transport plus a disruption of the cytoskeleton inhibits the exchanges of vital macromolecules and organelles; **f.** Disruptions in several stages of RNA metabolism, such as RNA processing, transport and utilization are a result of impaired function of hnRNP. Figure adapted from [49].

Even if presented as individual mechanisms, the pathogenic events are connected. Having various cellular mechanisms involved in the disease progression makes it extremely challenging to determine which are the most critical.

1.6.1. Dysregulated cellular mechanisms

1.6.1.1. Protein Aggregation and ER stress

Both FALS and SALS cases present misfolded proteins that originate protein aggregation in the cytoplasm of motor neurons and glial cells in several neurodegenerative diseases [50]. Several mutated genes in ALS like *SOD1*, *C9orf72*, *TARDBP*, and *FUS* give rise to protein aggregation. TDP-43 is the main protein that comprises aggregations in ALS and FTD cases [51]. In ALS there are three types of protein aggregates: ubiquitinated inclusions, Bunina bodies and hyaline conglomerates inclusions [52,53].

The accumulation of misfolded proteins causes endoplasmic reticulum (ER) stress and two adaptative pathways can become activated: the unfolded protein response and the ER-associated protein degradation pathway [54] (Figure 1.3a).

1.6.1.2. Abnormal RNA metabolism

Proteins FUS and TDP-43 are RNA-binding proteins (RBPs) that bind RNA molecules at specific sequences or secondary structures to facilitate several steps of RNA processing. Alterations in RBPs can lead to abnormal RNA splicing, transport, and stability (Figure 1.3f). Such defects are increasingly recognized as critical determinants of neurological diseases, such as ALS [55]. ALS-associated mutations in *FUS* and *TDP-43* change the dynamics of membrane organelles and accelerate fibrillization resulting in toxic properties [56].

Stress granules are composed of mRNAs and proteins that are formed as a consequence of cellular stress, being able to sequester specific unnecessary mRNAs inhibiting their translation. Disturbances carried out by mutant RNA-binding proteins can have damaging outcomes in stress granules consisting in alterations of its RNA material properties, impairing their function and contributing to the pathology [55].

1.6.1.3. Proteasome Inhibition and Autophagy

The ubiquitin-proteasome system (UPS) and the autophagy process (Figure 1.3a) are the major pathways for protein degradation. Various ALS-associated gene mutations encode proteins involved in these pathways, for instance *C9orf72*, *OPTN*, and *UBQLN2* [57–59]. In UPS, abnormal proteins are marked by ubiquitination to be identified and, consequently, degraded by the proteasome [60]. In *SOD1* ALS-associated mutations the overexpression of SOD1 proteins results in the inhibition of the proteosome due to saturation, leading to cell death [61]. Autophagy involves the formation of double membrane structures which fuse with lysosomes to degrade

proteins and recycle long-lived proteins. Mutations in the *UBQLN2* gene impair the transport of polyubiquitinated proteins to the proteosome or the autophagosome to be degraded. Mutations have also been observed in the protein optineurin which is a proposed receptor for autophagy [59].

1.6.1.4. Damaged Axonal Transport

The interaction between neurons requires functional axonal transport. Axonal transport includes the movement and spatiotemporal circulation of intracellular molecules performed by molecular motors of the dynein (retrograde transport) and kinesin (anterograde transport) families. Disrupted organization of the axonal cytoskeleton, particularly of the essential neurofilaments, is present in ALS [62]. Mutations in the p150-glued (DCTN1) subunit of dynactin (Figure 1.3e) have been described in ALS patients, significantly reducing the transport and promoting motor neuron disease [63]. Mutated TDP-43 protein impairs axonal transportation and so, delivery of essential mRNAs is disrupted in ALS as shown in several studies where mutated TDP-43 protein impairs axonal transportation of RNA granules in *Drosophila*, mouse cortical neurons and some stem cell-derived neurons from ALS patients [64].

1.6.1.5. Oxidative Stress

Oxidative stress in ALS induces damage to the organism, having a tendency to increase with age [65]. The process occurs when there is an unregulated production of reactive oxygen species (ROS) such as hydrogen peroxide, peroxynitrite, superoxide and hydroxyl radicals. The cell's antioxidant capacity is lower than the production of ROS in pathologies. There is evidence of oxidative damage in the spinal cord of SALS patients [66], as well as increased levels of a marker for oxidative stress [67]. Stimulation of excessive extracellular production of superoxide by microglia is a result of misfolded mutant SOD1 in association with GTPase RAC1, consequently dysregulating the NADPH oxidase activation (Figure 1.3b) [68].

1.6.1.6. Excitotoxicity

In ALS, neurons become damaged due to the excessive stimulation provided by glutamate receptors, either because levels of glutamate in neurons surpass normal levels or due to failure in quickly removing the synaptic glutamate present [49]. There are several proposals by which the dysregulation of glutamate occurs. It was been proposed that elevated levels are a consequence of the selective loss of the glial glutamate transporter 1 (GLT1), also called glutamate excitatory amino acid transporter 2 (EAAT2) [69], in the brain and spinal cord (Figure 1.3d). In addition, astrocytes release soluble factors that induce motor neurons to upregulate the glutamate receptor subunit glutamate 2 (GluR2) in neurons, reducing its calcium permeability and protecting the neurons. Pathologically, there is an incomplete editing of the pre-mRNA that forms GluR2. Thus, the AMPA receptor (ionotropic transmembrane receptor for glutamate)

becomes permeable to calcium molecules. Elevated calcium levels damage neurons due to the low expression of proteins able to bind calcium and control its levels [68], leading to cell death.

1.6.1.7. Mitochondrial Dysfunction and Apoptosis

Mitochondria change their function or even become dysfunctional prior to disease onset as seen in *in vivo* studies of ALS models [70]. Furthermore, studies show aggregated and dilated mitochondria present in SALS, plus immense mitochondrial vacuolation in mice with SOD1 mutations [71,72]. At disease onset there is defective synthesis of adenosine triphosphate (ATP) along with defects in complexes I and IV of mitochondrial respiration in the brain and spinal cords of mice with mutant SOD1 [73]. At the same time, high calcium levels released from mitochondria, as well as pro-apoptotic factors (cytochrome c) into the cytosol activate signaling cascades leading to apoptosis [74]. In ALS there is an increased activation of an apoptotic response, mainly of effector caspase-1 and caspase-9 [75,76]. The caspase-3 activation in glial cells has been shown to inactivate the EAAT2 transporter, pre-disposing neurons to excitotoxicity (Chapter 1.6.1.6) [77].

1.6.2. Neuroinflammation

In many neurodegenerative diseases including ALS, neuroinflammation is a common pathological aspect. Neuroinflammation corresponds to the activation of CNS resident glial cells such as astrocytes and microglia, as well as infiltration of the CNS by immune cells such as monocytes, neutrophils and lymphocytes which occur in infection, injury or degeneration [78].

Clear evidence of microglial activation has been found in gene mutations of proteins SOD1, TDP-43 and C9orf72 of ALS models, since they have been linked to promote proinflammatory-mediated motor neuron injuries either by inflammation or autophagy suppression [79].

Several studies were performed to understand the mechanisms underlying the disease onset and progression. While the exact mechanism is very complex and the onset is not exactly known, there is clear evidence that during ALS there is a constant inflammatory response mediated either by glia cells or the innate immune system. There is a stronger correlation to glia cells as the main “producer” of the neuro-inflammatory response.

In patients and animals with ALS, there is a clear activation of microglia and astrocytes found in the CNS system. It’s known that microglia activation induces the release of pro-inflammatory cytokines like TNF-alpha and interleukins (IL-1beta, IL-6, IL-12, etc). There is also evidence that neuroprotective activation could be expressed as well via expression of M2 microglia phenotype, through expression of CD206, IL-10, IGF-1. The inflammation could induce both a neurotoxic and neuroprotective effects, and depending on the M1/M2 phenotype ratio, they could either produce more impaired or dying motor neurons [80].

There is also impairment of the autophagy pathway during the pro-inflammatory response. Usually, autophagy restricts the generation of pro-inflammatory cytokines and mitochondrial production of reactive oxygen species. Some gene expressions like *SOD1*, *TARDBP* and *C9orf72* are linked to disruption of the autophagy pathway [81].

Mutant SOD1 mice models have shown the presence of neuroprotective anti-inflammatory mediators during the early phase of the pathology, combined with a conversion to a later stage marked by an increase in cytotoxic pro-inflammatory mediators [82,83]. As evidence, a study showed there was secretion of cytokine IL-6 (inflammatory cytokine) by activated macrophages and microglia in mutant SOD1 mice [84]. Additionally, in microglia the suppression of the mutant gene *SOD1* showed a relation between disease progression and SOD1 synthesis.

Evidence of decreased expression of mutant gene *C9orf72* in ALS patients and the loss of the referred gene is suggested to contribute to ALS pathology, since its deactivation in mice results in abnormal microglia and age-related neuroinflammation [85,86].

However, in TDP-43 and C9orf72 models, direct neurotoxic effects of pro-inflammatory microglia have not yet been conclusively demonstrated.

Mutations in *OPTN*, *TBK1*, and several other genes have been stated to directly compromise immune gene function and stimulate inflammatory responses in FALS [81], making them the clearest evidence that CNS and peripheral immune system that result in inflammatory mechanisms are involved in the pathogenesis of FALS.

Oligodendrocytes supply lactate to axons by activating the monocarboxylate transporter (MCT 1) (Figure 1.3c). Reduced expression of MCT 1 is present in ALS, plus there is an impairment of function as a result of mutant SOD1 [87]. Delay in disease onset occurred when the synthesis of mutant SOD1 was reduced early in oligodendrocyte maturation [88].

Astrocyte cells have many functions in the CNS, such as source of nutrients for MN as well as ion buffering and also recycling the neurotransmitter glutamate (chapter 1.6.6). When reducing mutant SOD1 synthesis in mice astrocytes, a slower onset and progression of disease occurred with the addition of a delay in microglial activation [89].

Glial cells-derived molecules can be detected and measured in CSF or in the peripheral blood of patients with the pathology, such as our molecule of interest, chitotriosidase (CHIT1). CHIT1 was observed to be expressed in both macrophages and microglia, and injection of the protein into rats was associated with increased microglial levels and activation, astrogliosis, release of pro-inflammatory cytokines and motor neuron loss [90].

1.6.3. Biomarkers

Although ALS is the most common form of motor neuron disease it remains without diagnostic, and when ultimately patients reach the clinical criteria for ALS, in addition with the

exclusion of other diagnosis, it is too late for the patient. Therefore, it is crucial to find an approach to detect ALS in patients.

Biomarkers are laboratory tests used to measure the alteration of biological pathways associated with a disease, making them a necessary tool to distinguish between pathologies, to monitor disease progression, perform patient stratification for clinical trials, and provide earlier diagnosis. Currently, ALS biomarker choices are derived from biological components such as human tissue, blood, cerebrospinal fluid (CSF), and urine. More specifically, recent biomarker molecules have involved protein aggregates [91,92], oxidative stress-related molecules [93], and a few others [94]. In addition, non-molecular approaches for biomarkers are based on electrophysiological and neuroimaging parameters [95].

Neurofilaments are closer to become the first molecular biomarker for ALS. They are abundantly present in axons, being released in case of neuroaxonal injury, consequently proceeding to the CSF, and at lower concentrations to the blood [96]. There are four subunits: neurofilament heavy chain (NfH), medium chain (NfM), light chain (NfL) and α-internexin [96].

There is evidence of abnormal levels of neurofilaments in neurological disorders, such as multiple sclerosis, Parkinson's disease, ALS, and others [97]. Numerous studies have confirmed the presence of higher levels of neurofilaments in patients with ALS in contrast with other diseases and mimics [98,99]. In addition, in early clinical phases there was detection of increased of NfL and NfH levels on both FALS and SALS [98,100,101]. A multicenter quality control evaluation of biomarker candidates concluded that the level of phosphorylated NfH (pNfH) in the CSF is the most promising biomarker candidate for routine measurements and a benchmark for the investigation of biomarkers in ALS [102]. However, further studies have also stated that CSF NfL and NfH, as well as serum NfL, may also be suitable for the differential diagnosis of ALS [103].

Interestingly, neurofilaments in blood were detected with the first clinical sign of ALS, and studies determined the presence of high NfL levels [104–107], while others showed high levels of NfH in the blood of ALS patients [108,109].

Additional analyses of neurofilament levels is required to define, through a universal handling of different performed tests and identical preanalytical handling of samples, stable values for both the diagnosis and prognosis of ALS [110,111]. Moreover, it would be of interest to determine whether neurofilaments levels in the blood can be used to stratify patient groups in clinical studies since it is an easier biological fluid to obtain compared to CSF. Unfortunately, neurofilaments levels are also increased in other neurological diseases, driving the need to find additional targets.

More recently, chitinases appeared as promising biomarkers for ALS.

1.6.3.1. Chitinases as new possible biomarkers for ALS

Chitinases from the family 18 of glycosyl hydrolases (GH18) are emerging as biomarkers in inflammatory and neurodegenerative disorders. Mammalian chitinases include the enzymatically active chitinases chitotriosidase (CHIT1), the acidic mammalian chitinase (AMCase), and the chitinase-like proteins (C/CLPs), such as chitinase 3-like 1 and -like 2

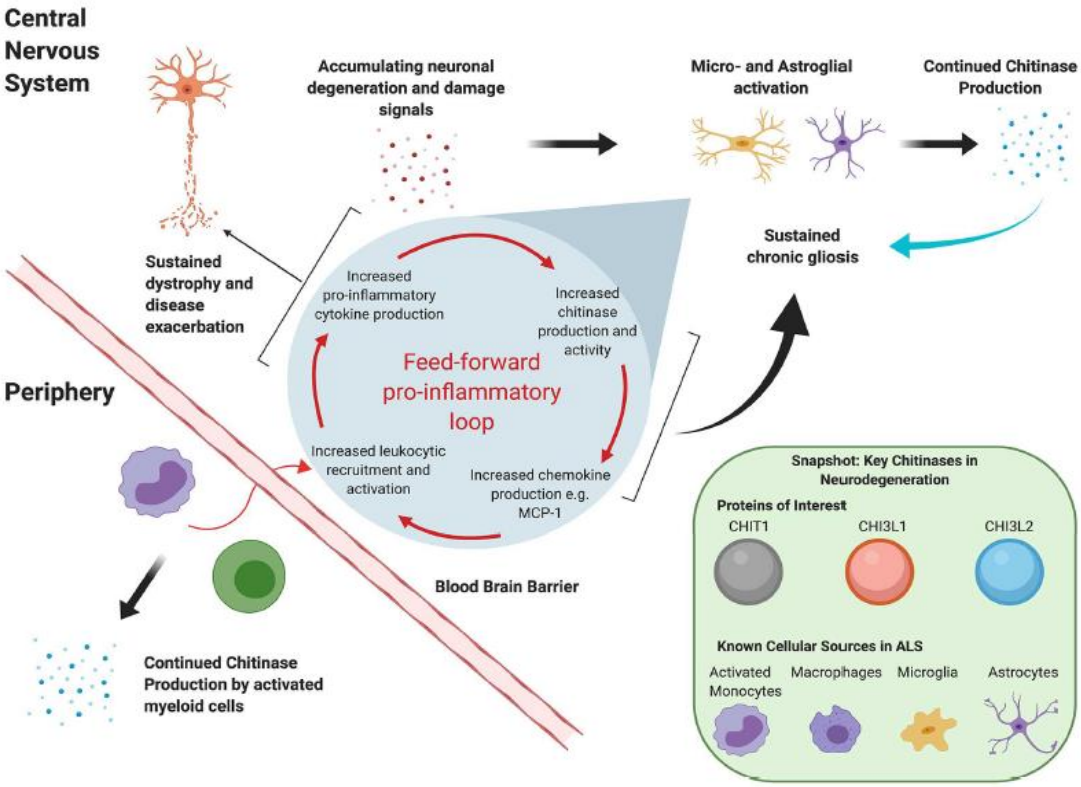

Figure 1.4- Synthesis of chitinases and their effects in the mammalian immune system contributing to neuroinflammation in ALS. Figure adapted from [112].

(CHI3L1, CHI3L2), oviductin-specific glycoprotein (OVGP1), and stabilin-1-interacting CLP (SI-CLP) [112]. Chitinases CHIT1 and AMCase are classified as "true chitinases", containing an enzymatically active domain that hydrolyzes chitin. Chitin is a linear polymer formed of β-(1-4)-poly-N-acetyl-D-glucosamine (GlcNAc) repetitions, being considered the second most abundant polysaccharide in nature. On the other hand, C/CLPs do not possess the ability to hydrolyze chitin, due to substitution of amino acids in the catalytic center [113].

There is no presence of endogenous chitin in mammals, however, a number of both C/CLPs and chitinases has been detected. Chitinases are produced in high amounts by the host to defend and clear chitin and chitinous organisms that cause infections [113], thus being involved in the innate immune response. Even though the roles of these molecules have not yet been clarified, there is indication that their function goes further than the activation of innate immunity against pathogens, also playing a role in inducing oligodendrogenesis for instance [41].

Chitinases and C/CLPs have been highly described as markers of neuroinflammation and reactive gliosis in a wide variety of neurologic disorders, even being proposed as prognostic biomarkers and therapeutic targets in some of the disorders, including ALS [112].

1.6.3.1.1. Chitotriosidase (CHIT1)

Chitotriosidase (CHIT1) is the best-characterized chitinase from both clinical and biological perspectives. It is mainly expressed by cells of myeloid lineage, especially from infiltrated peripheral macrophages on several causing stimulus [114,115], neutrophils granules [116] and monocyte-derived cells, Kupffer cells, osteoclasts, and dendritic cells [117]. *CHIT1* gene is located in the chromosome 1q32.1, having 13 exons and around 20 kb to encode a 445 amino acid long protein and exists in two isoforms: a full-size 50 kDa (secreted isoform) or a 39 kDa lysosomal isoform (with only the catalytic domain) [118]. CHIT1 is thought to be important in the regulation of inflammation [119] as well as a mediator of the innate immune response [113].

CHIT1 was proposed as a CSF marker of microglia activation in ALS sustaining neuroinflammation and therefore, aggravating the pathology [120], since it was detected in microglia from the corticospinal tract, in macrophages and neutrophils [121].

In an early report, using quantitative mass spectrometry (MS) and enzyme-linked immunosorbent assay (ELISA) levels of CHIT1 were found to be significantly higher in ALS patients when compared to healthy controls in the CSF [122]. Another study provided evidence of higher levels of CHIT1 in CSF of ALS patients when comparing to not only healthy controls, but to mimics, and symptomatic mutation carriers, and that the increased CHIT1 levels corresponded to the active form of the protein [123]. Even so, further studies are needed since CSF CHIT1 levels are still outperformed by neurofilaments, plus only a weak distinguishedness was found between levels of CHIT1 from ALS and PLS [112], also because CHIT1 levels are also increased in other neurodegenerative diseases [110,120].

Studies have also aimed to find links between high CHIT1 levels in the CSF with the patients' clinical parameters, and so far associations with disease severity (overall ALSFRS-R score) [124], disease progression rate (PR) [111,120,125], survival and mortality [120], and disease duration [110,123] have been reported. Interestingly, the only correlation found so far regarding the respiratory parameters of ALS, was with the respiratory function index forced vital capacity (FVC) [121].

Recently, elevation of CHIT1 levels was found in a more accessible biofluid, blood (plasma or serum). Studies about CHIT1 levels in the blood of ALS patients have not been in agreement. One particular study showed CHIT1 activity was higher in dry blood samples of ALS patients [126]. In addition, a significant increase of blood CHIT1 levels was reported in one cohort of genetic patients with ALS [127]. On the other side, contrary to the previously mentioned

allegations, the latest studies have shown that the detected difference in blood CHIT1 levels in ALS is not significant [123–125].

Attempts to link the levels with the prognostic parameters were possible in one study, correlating CHIT1 levels in dry blood with FVC [126], while other correlations were not successful.

Remarkably, it was possible to correlate blood chitinases levels with established neurodegenerative markers, including the neurofilaments [110,111,127]. In this study, further investigation of this more accessible biofluid marker, blood CHIT1, is taking place while also taking special interest in finding correlations between plasma CHIT1 levels and respiratory parameters of ALS patients.

1.7.Objectives

The present work aimed at investigating two proteins involved in the pathogenic mechanisms in ALS. The first was CHIT1, a chitinase induced in neuroinflammation, that has emerged as a promising disease biomarker from the cerebrospinal fluid. The second was GLT8D1 a glycosyltransferase that was recently found mutated in some families with ALS.

The first objective consisted of the quantification of CHIT1 from plasma samples in order to test its biomarker potential for ALS. With that purpose, an ELISA assay has been developed. Comparison between ALS patients and healthy controls as well as correlations with patients demographic and clinical parameters, including respiratory parameters, have been investigated.

The second objective involved the analysis of GLT8D1, including its N-glycosylation type. Elucidation of the *in vitro* specificity of the enzyme towards monosaccharides, oligosaccharides and N-glycans has also been performed using a luminescent Universal Glycosyltransferase Activity Assay complemented with mass spectrometry analysis.

2. Material and Methods

2.1. Plasma samples

Blood was collected to a tube containing ethylene-diaminetetra-acetic acid, centrifuged at 1000x*g*, 10 min and the remaining supernatant consisting of plasma was stored at -80 °C. In this study a set of 40 ALS identified patients (28 males and 12 females) and 11 controls (4 males and 7 females) without any neurological disease (Table 2.1).

Table 2.1- Demographic and clinical features of the patients included in the study. Median and interquartile ranges are shown. *median age was calculated with 4 controls and 40 ALS patients **respiratory subscore of the ALSFRS.

	Gender (F/M)	**Age* (years)**	**Disease duration (years)**	**ALSFRS**	**Respiratory subscore****	**Onset site (bulbar/spinal /axial)**	**Age at onset**	**Rate of disease progression**	**CHIT1 (pg/mL)**
Controls	7/4	56.7 (39.2-62.6)	-	-	-	-	-	-	20017 (12804-35794)
ALS	12/28	65.3 (56.3-72.6)	1.13 (0.74-1.48)	31 (23-34)	11 (9.25-12)	(14/25/1)	64.3 (55.1-69.8)	0.81 (0.35-1.33)	33621 (19753-66795)

All gave informed consent as required by the local Ethics Committee before blood collection. The subjects included were regularly followed at the Neuromuscular Unit of the Department of Neurosciences (Hospital de Santa Maria, Lisbon). All ALS patients progressed to a probable or definite disease, according to the revised El Escorial criteria [3]. At the time of sampling the patients disease severity was scored by applying ALSFRS and the respiratory subscore of ALSFRS. The research protocol respected the Declaration of Helsinki on ethical principles for medical research involving human subjects.

2.2. Plasma chitotriosidase quantification

Chitotriosidase from plasma was quantified using sandwich enzyme-linked immunosorbent assay (ELISA).

Initially, 96-well plates (ThermoFisher Scientific-Nunc MaxiSorp 96 flat-bottom, (ref.44-2404) were incubated overnight at 4 °C with 1.5 μg/mL of coating affinity-purified polyclonal goat IgG antibody (R&D systems, AF3559) diluted in coating buffer (0.2 M sodium carbonate/bicarbonate pH 9.4) to a total of 50 μL per well. Blocking was done with 300 μL of blocking solution per well (1% casein in PBS, Bio-Rad, 1601783) for 1h at room temperature. Then, 50 μL of standard recombinant human CHIT1 (expressed in HEK 293 cells, Sigma SAE0052) were added (range 0 to 3600 pg/mL) and incubated for 1h, to perform the calibration curves. For quantification, in parallel, 50 μL plasma samples (diluted in blocking buffer 1:50 or 1:75) previously centrifuged at 10000xg at 4°C for 10 min, were added to the wells. After

washing, plates were incubated with 0.75 μg/mL of biotinylated mouse monoclonal IgG1 detection antibody (from mouse myeloma cell line N20-derived recombinant human CHIT1 R&D systems, MAB3559) for an additional hour. After washing, plates were incubated with 50 μL enzyme conjugated anti-mouse IgG (horseradish peroxidase-linked whole antibody, 1:500; GE Healthcare, NA931), diluted in blocking solution for 1 hour. For detection, 50 μL of substrate solution 3,3',5,5'-tetramethylbenzidine (TMB) (ThermoFisher, N301) were added per well. After 30 min, 50 μL 2 M sulfuric acid was added to stop the reaction. Each condition was performed in duplicate. All washes were performed using 200 μL of 1X PBS, 0.05% Tween-20 three times for 5 min each. Measurements were obtained with a Tecan infinite F500 microplate reader.

Plasma CHIT1 concentration was determined from interpolation in a four-parameter logistic (4PL) non-linear regression curve of concentration versus absorbance (A450 – A550) using GraphPad Prism 9.

Normality was checked by D'Agostino and Pearson omnibus normality test and sample distributions were not normal. CHIT1 concentration was presented as a median and the interquartile range (IQR, 25–75% percentiles). Progression rate was calculated as (40-ALSFRS)/disease duration. Statistical comparisons applied nonparametric Mann–Whitney test and Spearman's non-parametric correlation analysis. Receptor operator characteristic (ROC) curve analysis was performed, and area under the curve was (AUC) calculated.

In statistics, *p* value gives the probability of any observed difference having happened by chance, being classified from significant, highly, very highly and not significant (0.05, 0.01, 0.001, > 0.05, respectively), the lower the *p* the greater the statistical significance of the observed difference. Values of $p < 0.05$ were considered significant.

Another value of interest is the correlation coefficient (r) of a linear relationship between two variables, being either a positive or a negative correlation and varying from very low to very high correlation (r = 0 to 0.2; r = 0.8 to 1.0, respectively).

Statistical analysis was conducted with GraphPad Prism 9 (GraphPad Software, San Diego, CA, USA).

2.3. Protein extraction

HEK-293 cells were extracted to obtain full-length membrane GLT8D1, either the wild type (flGLT8D1-wt) or the mutant R92C form (flGLT8D1-R92C), with Triton X-100 buffer (50 mM Tris-HCl pH 7.5, 150 mM NaCl, 1 mM ethylenediamine tetraacetic acid-EDTA), 1% (w/v) Triton X-100, 0.02% protease inhibitors cocktail- Roche) for 30 min on ice with occasional vortex. The extract was then centrifuged at 10000x*g* at 4 °C for 10 min, in order to remove insoluble material, and the supernatant collected.

2.4. Protein Quantification

Total protein was determined by the bicinchoninic acid method (BCA). A calibration curve between 0 and 25 μg/mL was developed using bovine serum albumin (BSA) as standard protein, and protein concentration was calculated by interpolation. The standards and the samples were left to precipitate with 10% (w/v) trichloroacetic acid (TCA) and 1% (w/v) sodium deoxycholate (DOC) for 10 min. After a centrifugation at 10000x*g* for 10 min, a solution of BCA:Cu(II)SO_4 (Sigma-Aldrich, BCA1) 50:1 was added to the resulting pellet. The samples were incubated at 37 °C for 30 min.

The absorbance was then measured at 562 nm with Spectrophotometer UV-1603 UV-VIS (Shimadzu).

2.5. SDS-PAGE and Immunoblotting

GLT8D1 was studied as a secretory soluble form (sGLT8D1) and full-length membrane bound forms. Secretory sGLT8D1 was kindly provided by Professor Kelley Moremen [128] from the Complex Carbohydrate Research Center, University of Georgia, Athens, USA. This protein included the catalytic domain and several fusion tags and was produced from HEK-293 cells (Figure 2.1A). Full-length GLT8D1-wild type (flGLT8D1-wt) and mutant (flGLT8D1-R92C) were purified from HEK-293 cells overexpressing the enzyme (kind gift of Professor J. Cooper-Knock and Professor P. Shaw from Sheffield Institute for Translational Neuroscience (SITraN), University of Sheffield, UK) [31]. Full-length GLT8D1 forms had FLAG-Tag at the C-terminus for purification and detection of the protein (Figure 2.1B).

(A)

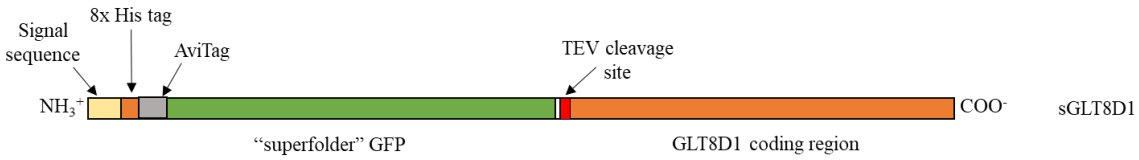

(B)

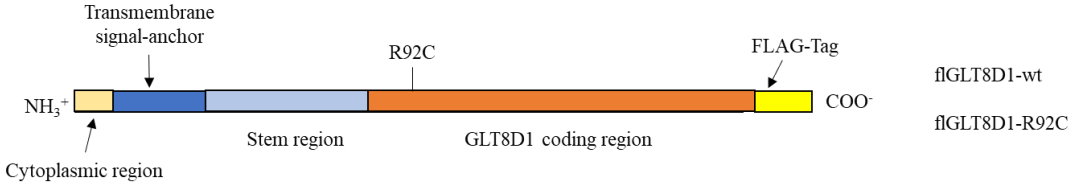

Figure 2.1- Identified structural and topology domains of both GLT8D1 forms used for analysis
(A) soluble GLT8D1: N-terminal signal sequence was replaced by a tobacco etch virus (TEV) protease recognition and cleavage site sequence. After gateway recombination and selection cassette was replaced with the glycoenzyme coding sequence, fusing with vector-encoded tag sequences (pGEn2 containing a signal sequence, an 8x His Tag, an AviTag and a GFP domain) took place. Purification of recombinant enzymes was done by immobilized metal affinity chromatography (IMAC); **(B) full-length GLT8D1** wild type and mutant R92C, including the site of identified mutation R92C in exon 4, available in the laboratory and purified from HEK-293 cells overexpressing the enzyme, and an FLAG-Tag in C-terminal for enzyme purification and detection.

Both GLT8D1 were analysed by sodium dodecyl sulphate polyacrylamide gel electrophoresis (SDS-PAGE), 10% and 12% of acrylamide (Mini-PROTEAN® TGX™ Precast Protein Gels, Bio-Rad). Proteins were denatured in reducing sample buffer **(**lithium dodecyl sulfate at pH 8.5 with SERVA Blue G250 and phenol red, plus 50 mM dithiothreitol (DTT) (NuPAGE™, Ref.: NP0007 and NP0004) and heated at either 70 °C for 10 min or 90 °C for 5 min. Protein marker II (NZYTech, MB090) was used as a molecular mass marker. Samples were applied to the gel with a Microliter syringe (Hamilton, 50 mL) and the gels were run in an electrophoretic chamber (Bio-Rad), in running buffer at 180 V for approximately 40 min. Gels were stained with Coomassie Blue R-250 (Merck, ref.: 42660) and destained with a solution of 50:40:10 (methanol:H_2O:acetic acid).

For immunoblotting, proteins were transferred to polyvinylidene fluoride membranes (PVDF) that after words were immediately blocked with 5% non-fat dry milk (Nestlé) in Tris-buffered saline (TBS) (20 mM Tris-HCl pH 7.5, 150 mM NaCl) with 0.1% (w/v) Tween-20 (TTBS) for 1 h. Tween-20 was used to avoid non-specific binding of proteins to the PVDF membrane. The membranes were incubated with the primary antibodies overnight at 4 °C, and later with the secondary antibodies coupled to horseradish peroxidase (HRP) for 2 h at room temperature. The antibodies used are specified in Table 2.2. Washes were with TTBS, applied after the primary and secondary antibodies, four times for 5 min each. Detection was performed with the Immobilon Western chemiluminescent HRP substrate (Millipore, WBKLS0500). Oxidation of luminol releases energy in the form of light when oxidized by hydrogen peroxide, coupled to the secondary antibody.

Image acquisition was done in Chemidoc XRS Imaging System (Bio-Rad) or iBright FL 1500 Imaging Systems (Invitrogen).

Table 2.2- Antibodies with respective dilution and buffer conditions used in immunoblotting analysis.

Antibodies	Dilution	Buffer	Supplier
Mouse anti-FLAG M2 monoclonal	1:4000	5% non-fat dry milk in TTBS, 0.02% NaN_3	Sigma-Aldrich F3165

Mouse anti-His Tag IgG1 monoclonal	1:7000	5% non-fat dry milk in TTBS, 0.02% NaN_3	GenScript A00186
Mouse anti-His Tag IgG1 monoclonal	1:5000	5% non-fat dry milk in TTBS, 0.02% NaN_3	GenScript A00186
Rat anti-GFP IgG2a monoclonal	1:500	5% non-fat dry milk in TTBS, 0.02% NaN_3	Chromotek 3h10
Rabbit anti-GLT8D1 polyclonal	1:1000	5% non-fat dry milk in TTBS, 0.02% NaN_3	Sigma-Aldrich HPA010588
Goat anti-rat IgG coupled to HRP	1:5000	5% non-fat dry milk in TTBS	Pierce
Sheep anti-mouse IgG coupled to HRP	1:3000	5% non-fat dry milk in TTBS	GE Healthcare NA391

2.6. GLT8D1 deglycosylation

In order to investigate the presence of glycans in the protein structure, proteins were deglycosylated with the enzymes peptide N-glycosidase F (PNGase F) and endoglycosidase H (Endo-H) that can effectively remove N-glycans from glycoproteins resulting in a mobility change of one or more of the bands on the SDS-PAGE gel. Each enzyme is specific to a site in the protein as shown in Figure 2.2.

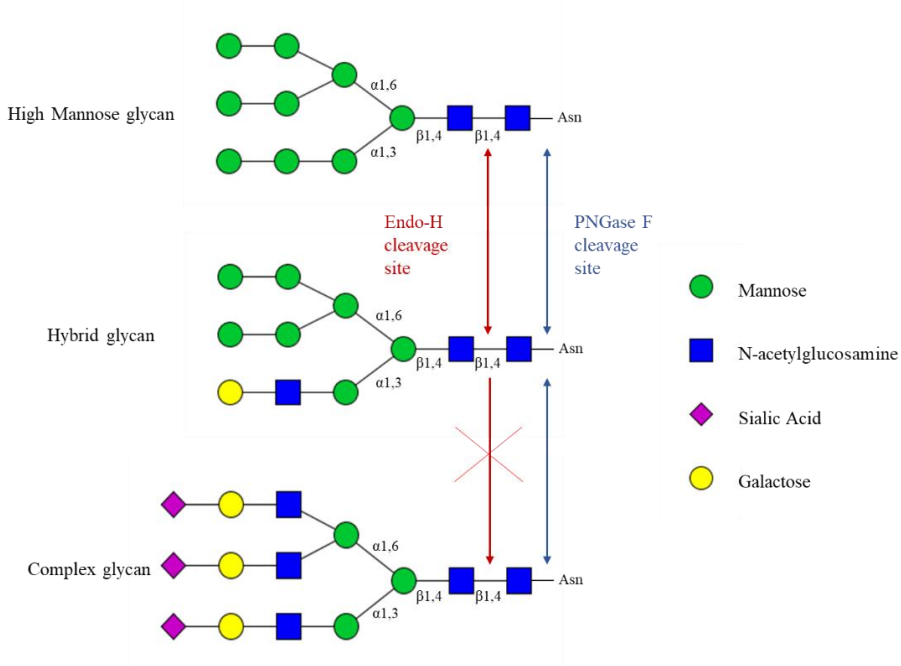

Figure 2.2- Schematic representation of enzymatic action of PNGase F and Endo-H with their respective specificity cleavage sites in each the three types of glycans.

For GLT8D1 hydrolysis of N-glycans, samples were incubated with 2% SDS, 10% β-mercaptoethanol and 0.02% protease inhibitors cocktail (Roche) at 99 °C for 5 min. After cooling down, the samples were incubated overnight at 37 °C with 2.5 or 5 mU (0.5 or 1 µL) Endo-H (Roche, 11 088 726 001) in 50 mM sodium citrate pH 5.5.

Using PNGase F, samples were incubated with 0.1% SDS, 50 mM β-mercaptoethanol and 0.02% protease inhibitors cocktail (Roche) at 99 °C for 5 min. Later 1.25 or 2.5 mU (1 or 2 µL) of PNGase F (Roche, 11 365 169 001) in 50 mM sodium phosphate pH 7.2 with 12.5 mM EDTA and 50% glycerol (v/v) and 0.75% (w/v) Nonidet P-40 was added.

2.7. Enzymatic activity of GLT8D1

GLT8D1 glycosyltransferase activity was measured using UDP-Glo™ Glycosyltransferase Assay kit (Promega Corporation, V6971). GLT8D1 transfers a sugar from a UDP-sugar substrate donor, UDP-galactose, to an acceptor molecule. The released UDP from the reaction converts to ATP, generating light in a luciferase catalyzed reaction (Figure 2.3A). Luminescence is then correlated to UDP concentration, and the light output is proportional to UDP concentration.

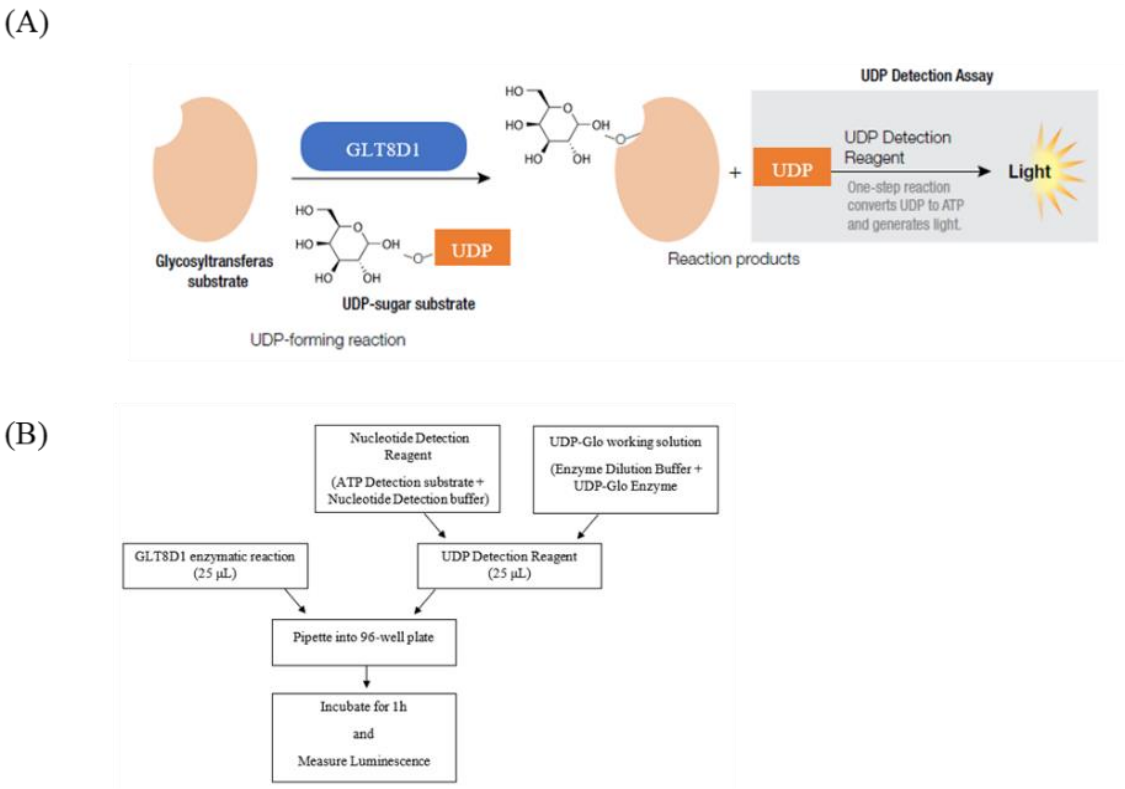

Figure 2.3- UDP-Glo™ Glycosyltransferase assay principle. **(A)** The UDP Detection Reagent is added to convert UDP to ATP and allow newly synthesized ATP to be measured using luciferase reaction. The light generated correlates with the amount of UDP produced by the GLT8D1 enzyme, which is indicative of its activity. After Promega protocol technical manual. **(B)** Schematic representation of the UDP-Glo™ Glycosyltransferase assay protocol using enzyme GLT8D1.

Following manufacturer recommendations (Figure 2.3B), standard curve was obtained in 1X glycosyltransferase buffer from samples from 0 to 25 μM UDP-standard (provided by the kit), to determine the relationship between UDP concentration and luminescence measurement.

Milk galactosyltransferase (GalT; Sigma, G5507) was tested in 35 μL reaction mixtures containing 50 mM Tris-HCl pH 7.5, 5 mM MnCl2, 0.03 U/mL GalT, 0.2 mg/mL α-lactalbumin, 20 mM glucose (Glc), and 0.1 mM ultra-pure UDP-Gal (Promega Corporation, V7171). Incubation was for 2 h at 37 °C. One unit of enzyme activity (U) was defined as the amount of enzyme that catalyzed the transfer of 1 μmol of Gal/min to the acceptors at 37 °C.

sGLT8D1 was tested in 35 μL reaction mixtures containing 50 mM Tris-HCl pH 7.5, 5 mM MnCl2, 0.1 mM ultra-pure UDP-Gal, 0.5 μL sGLT8D1, and several sugar acceptor substrates (presented in appendix Table 1 with respective concentrations). Incubations were in general for 16 h at 37 °C.

After incubation, 25 μL of mixture were transferred to wells in white 96-well plates (96 Flat Bottom White Polystyrene Costar, 3912) and 25 μL of UDP detection reaction were added to each well of the assay plate. Plates were mixed for 30 s on a shaker and incubated in a dark environment at room temperature for 1 h. Luminescence was recorded using microplate reader Tecan Infinite 200 PRO.

2.8. UHPLC-MS sample analysis

Molecule identification was characterized by Ultra High Performance Liquid Chromatography - Mass Spectrometry (UHPLC-MS) analysis using a Q-Exactive Focus (Thermo Scientific) coupled to a Dionex Ultimate 3000 UHPLC, using Xcalibur software v.4.0.27.19 (Thermo Scientific). The separation was achieved in a Thermo Hypercarb column (2.1x100 mm, 3 particle size, P/N 36003-102130), using a gradient of increasing percentage of 0.1% formic acid in acetonitrile and decreasing percentage of 0.1% formic acid in water. The flow rate was 0.4 mL/min, and the column was kept at 30 °C.

The method consisted of several cycles of Full MS scans (R=70000; Scan range=75-1125 m/z) followed by 3 ddMS2 scans (R=17500; 30 NCE) in positive mode. External calibration was performed using LTQ ESI Positive Ion Calibration Solution (Thermo Scientific).

Generated mass spectra were processed using Compound Discoverer 3.2 (Thermo) for small molecule identification. The search was performed against the Mass list provided, the mzCloud MS2 database, as well as the KEGG database. Mass spectrometry analysis was done by Conceição Almeida e Catarina Correia from the Mass Spectrometry Unit (UniMS), ITQB/iBET, Oeiras, Portugal.

3. Results

3.1. CHIT1 levels from the plasma of ALS patients

3.1.1. Development of a sandwich ELISA assay for CHIT1 quantification

A sandwich ELISA assay has been developed to quantify CHIT1 in the complex mixture of plasma. With that purpose, the concentrations of capture antibody, detection antibody and enzyme conjugate antibody, as well as blocking conditions, have been tested. The capture antibody used was polyclonal goat Ig G antibody in the range 0-10.54 µg/mL and the detection antibody consisted of monoclonal mouse Ig G1 antibody in the range 0-5 µg/mL (Figure 3.1). Enzyme conjugate antibody concentration was 1:1000. Blocking was with 1% casein in PBS. Commercial purified CHIT1 was used as standard for quantification. There was an increase in absorbance with increasing concentration of capture antibody that started to stabilize at approximately 3 µg/mL for concentrations of detection antibody below or at 2.5 µg/mL. On the other hand, the signal intensity also increased with increasing concentration of detection antibody, which started to stabilize around 1.25 µg/mL.

(A)

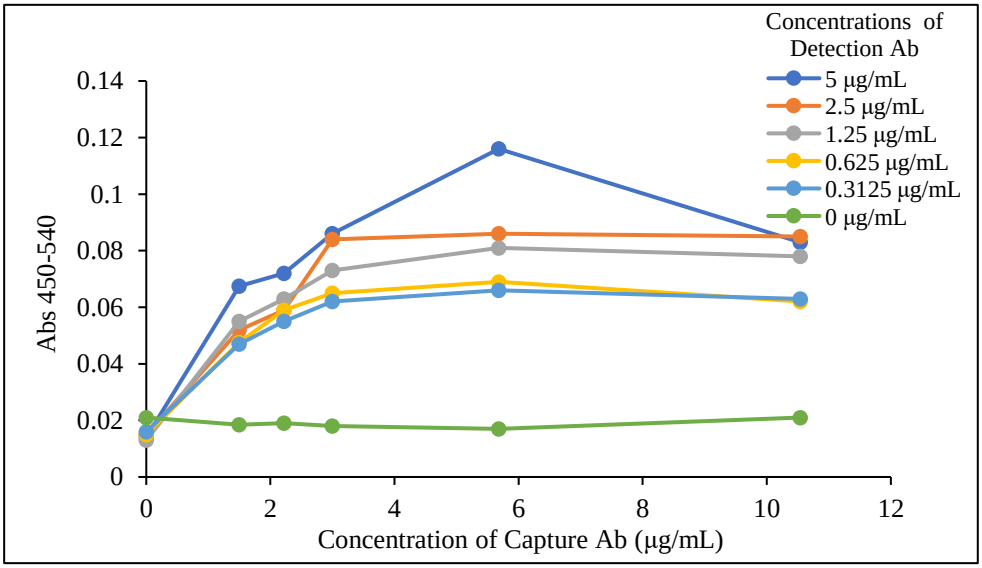

(B)

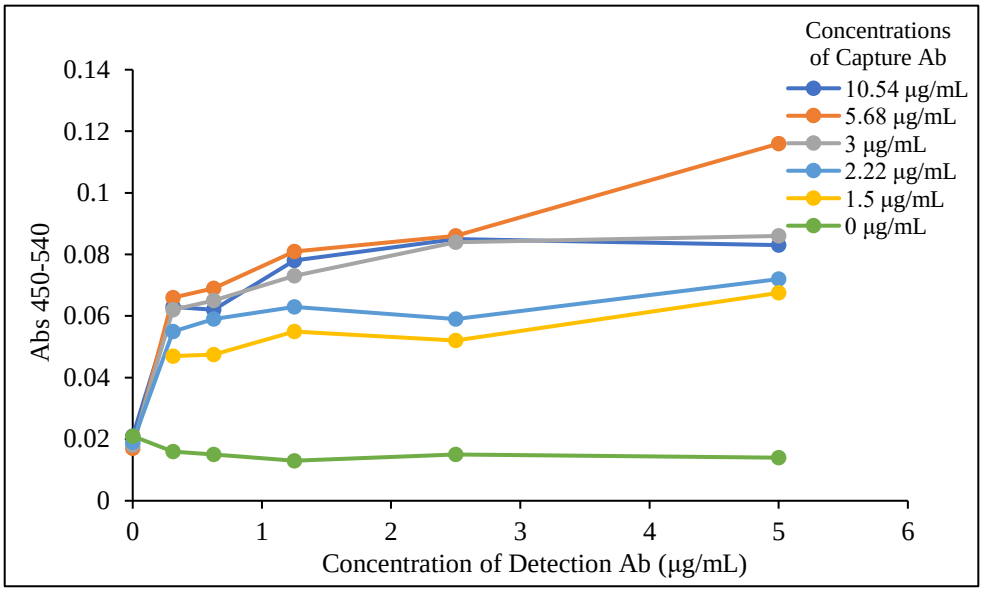

Figure 3.1- Variation in absorbance with the concentration of capture (A) and detection (B) antibodies used. Concentration of enzyme conjugate antibody used was of 0.64 µg/mL (dilution of 1:1000). Commercial CHIT1 standard from Circulex used at a concentration of 450 pg/mL.

Then, the assay was repeated using lower antibody concentrations tested before for confirmation (Figure 3.2). The combination of capture and detection antibodies at 1.5 and 0.75 µg/mL concentrations were selected for the subsequent assays. In this condition the signal was well-detected, and it was almost stable, particularly, for the detection antibody.

(A)

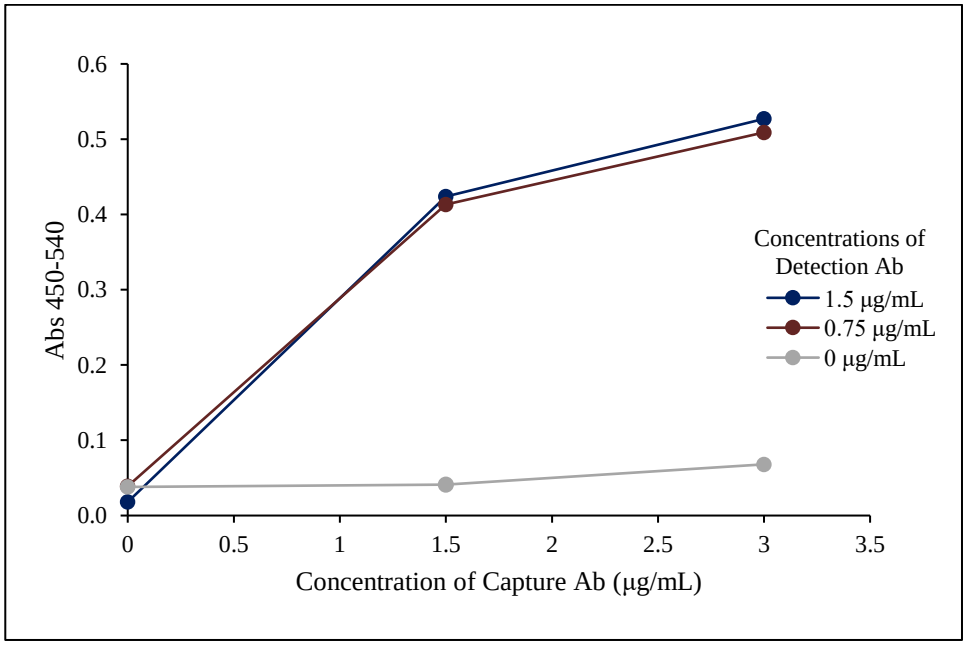

(B)

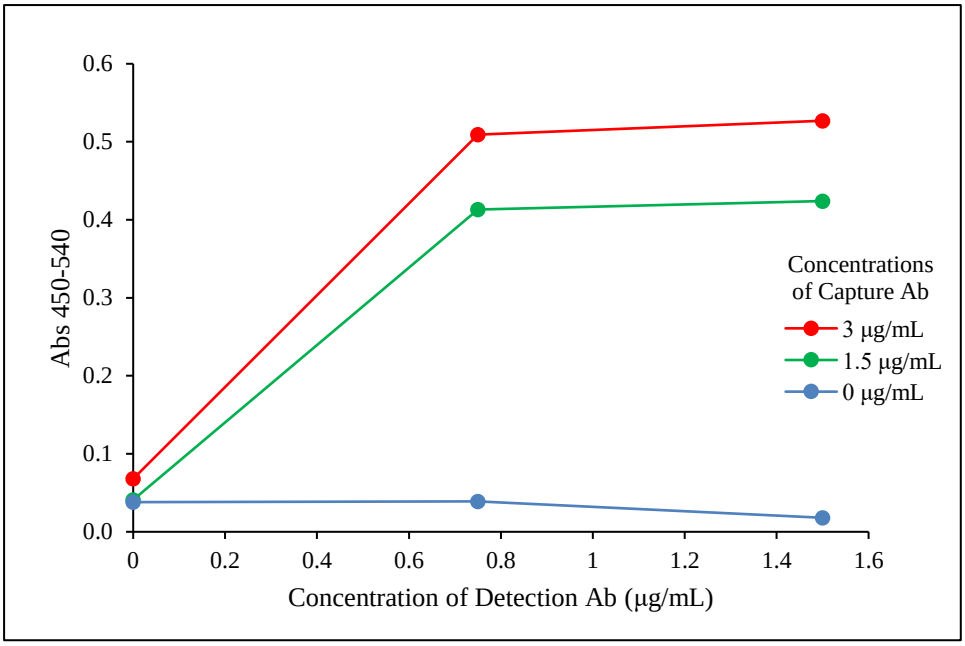

Figure 3.2- Variation in absorbance with the concentrations of capture (A) and detection (B) antibodies used. Concentration of enzyme conjugate antibody used was of 1.28 µg/mL (dilution of 1:500). Commercial CHIT1 standard from Circulex used at a concentration of 450 pg/mL.

Using the established conditions, three concentrations of enzyme conjugate antibody were tested (Figure 3.3). The enzyme conjugate antibody at 1.28 µg/mL (dilution of 1:500) was found to be adequate.

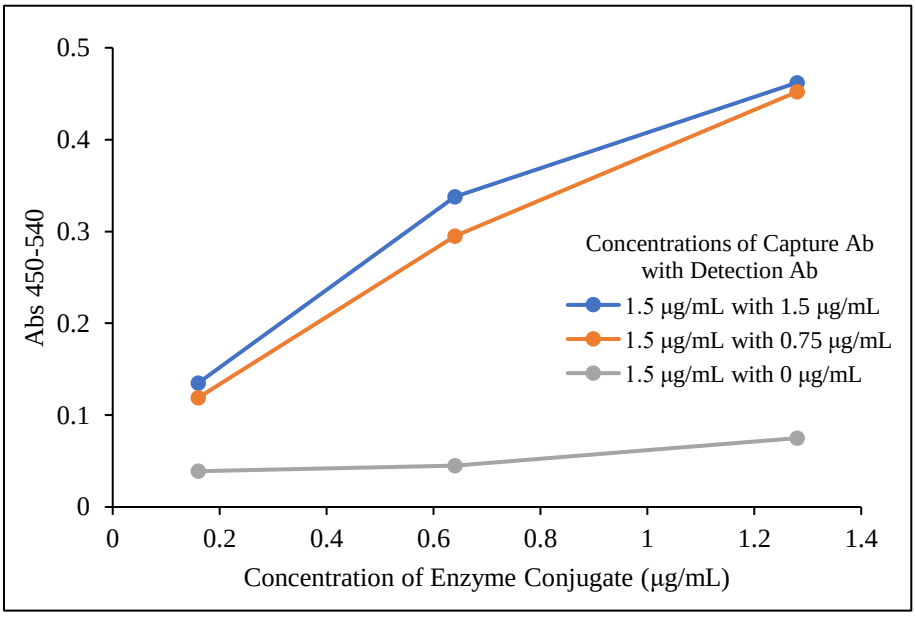

Figure 3.3- Variation of enzyme conjugate antibody concentrations with several combination between capture antibody and detection antibody. Commercial CHIT1 standard from Circulex used at a concentration of 450 pg/mL.

Using the selected conditions, a calibration curve with purified commercial chitotriosidase from Sigma as standard was established (Figure 3.4) using a four-parameter logistic (4PL) non-linear regression (GraphPad). The correlation coefficient of the curve was high (R^2=0.999).

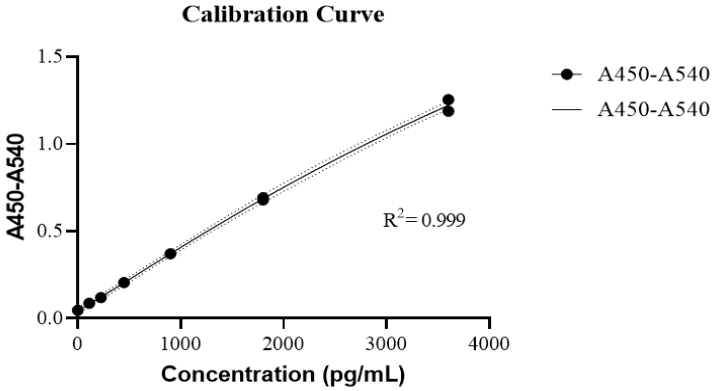

Figure 3.4- Calibration curve using commercial purified CHIT1 (Sigma). Measurements were performed in duplicate. Analysis done with GraphPad software.

The established assay was used to quantify CHIT1 from plasma of patients with ALS and controls by interpolation in the calibration curve. Plasma needed to be diluted 1:75 or 1:50 so that the CHIT1 concentration of the patients samples would meet this criterion.

To evaluate if the presence of plasma would interfere with the assay, a spike experiment was performed. In this assay a known amount of standard CHIT1 (72 or 108 pg) was added (spiked) into a plasma sample (dilution 1:75), and the corresponding concentrations were calculated. It was observed that the presence of plasma components did not interfere with CHIT1 quantification by this method.

3.1.2. CHIT1 levels from the plasma of ALS patients

In this study a group of 40 ALS patients and 11 healthy controls were studied (Table 2.1). Age between groups was higher in ALS patients than in controls but not significantly different, with a median of 65.3 (n=40) and 56.7 (n=4), respectively, and p = 0.099. Regarding ALS patients, clinical information was collected such as the onset site of disease in patients, where 14 had bulbar onset, 25 had spinal onset being the majority, and 1 had axial onset. Rate of disease progression was calculated through a formula using ALSFRS score and the years with disease, resulting in a median of 0.81. A standardized process is to monitor the respiratory subscore of ALSFRS, which resulted in a median of 11. Additional clinical information can be found in Table 2.1.

CHIT1 from the plasma of the investigated subjects was quantified using the developed ELISA assay. The median level of CHIT1 was 1.7-fold higher in ALS patients (33621 pg/mL) than in healthy controls (20017 pg/mL), but the difference did not reach statistical significance

(p = 0.083) (Table 2.1; Figure 3.5A). ROC curve analyses showed that the diagnostic performance of CHIT1 was poor with an area under the curve (AUC) of 0.67 (95% CI 0.53 to 0.85) and p = 0.081 (Figure 3.5B).

CHIT1 was quantified in follow-up of three patients. However, the results were not conclusive since there was no consistent change in plasma CHIT1 levels throughout visits.

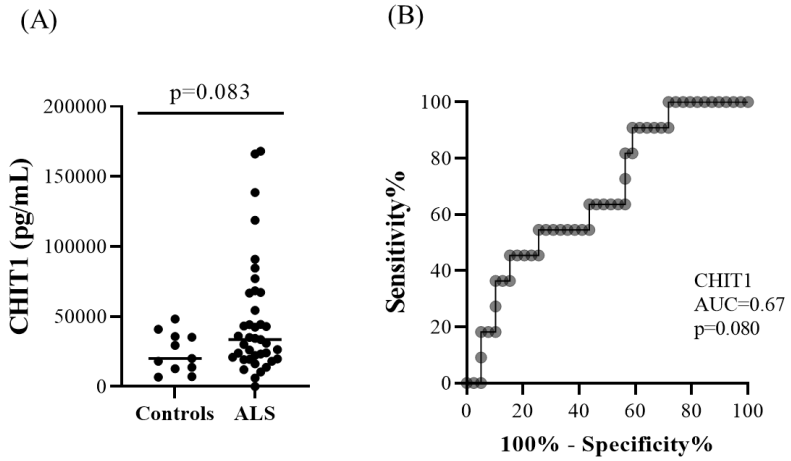

Figure 3.5- Levels of CHIT1 from plasma of ALS patients and controls. (A) Comparison of CHIT1 concentration in ALS patients and healthy controls. (B) ROC curve analysis of plasma CHIT1 where AUC represents area under the curve.

Possible correlations between CHIT1 levels and demographic information as well as clinical parameters of ALS patients, namely, age at sample, onset age, years with disease, ALSFRS, respiratory subscore, progression rate, FVC, partial pressure of carbon dioxide (pCO_2), and oxygen saturation (sPO_2) were investigated and are represented in Figure 3.6. The correlation values determined were low and non-significant.

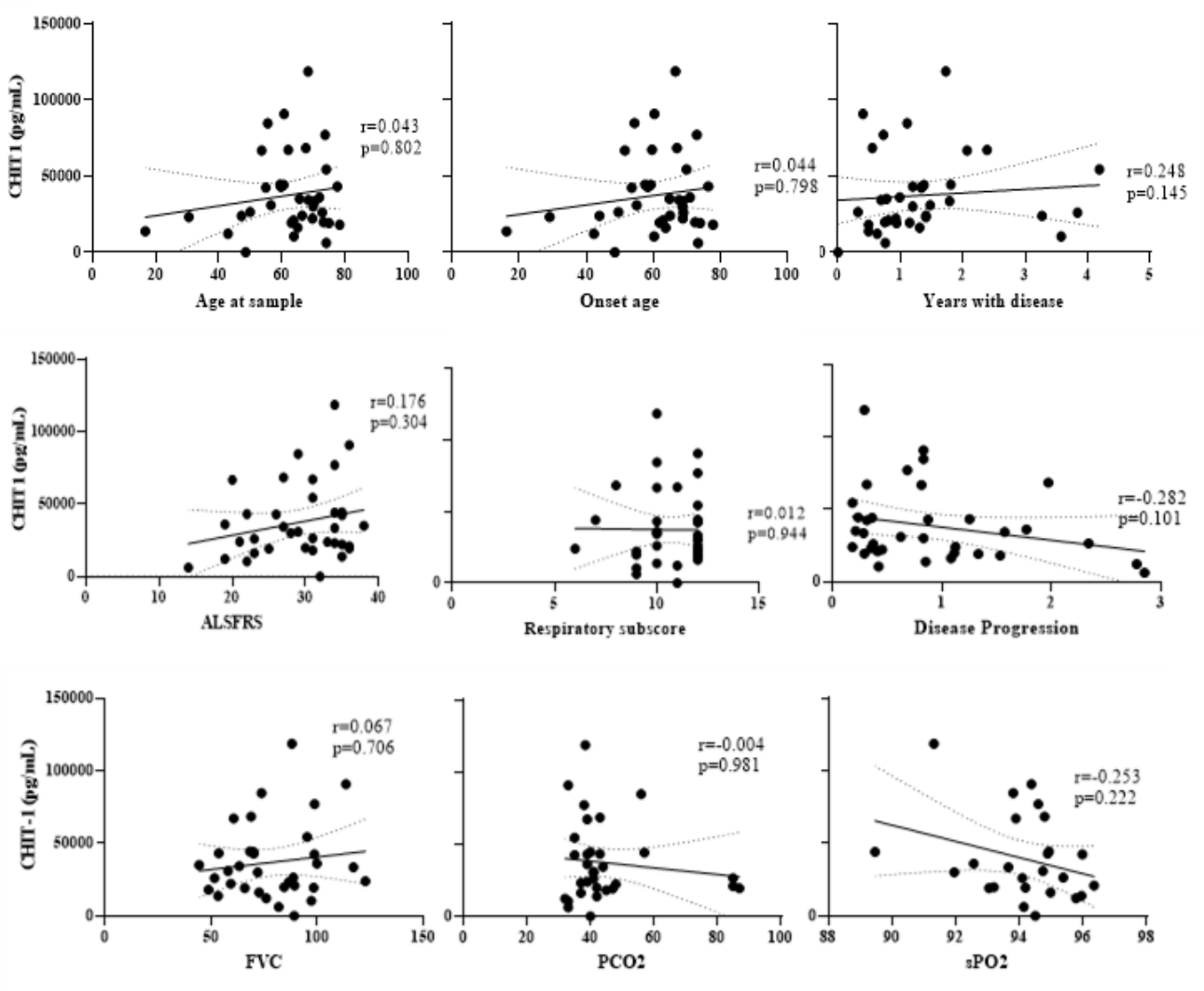

Figure 3.6- Correlations of CHIT1 from plasma of ALS patients with clinical parameters. Values classified as outliers were not considered for the calculations in the parameters.

3.2. Characterization of GLT8D1

3.2.1. Protein characterization

Full-length wild-type (flGLT8D1-wt) and mutant (flGLT8D1-R92C) GLT8D1 from HEK-293 cells (Figure 2.1 from Material and Methods) were analysed by immunoblotting. Both forms appeared at an apparent molecular mass slightly above 48 kDa (Figure 3.7). The predicted mass considering the amino acid sequence from UniProt (entry Q68CQ7) is 42 kDa. The difference in mass can be attributed to the FLAG tag at the C-terminus of the recombinant protein and to post-translational modifications, more specifically, N-glycosylation.

Then, it was investigated whether the R92C mutation, where an arginine is replaced by a cysteine, would lead to the dimerization of GLT8D1-R92C via disulfide bridges. With that purpose, SDS-PAGE was performed in non-reducing conditions (Figure 3.7). The results showed that Cys-92 from the mutant did not mediate the formation of dimers. Furthermore, no other oligomers were observed for either the wild-type or the mutant forms.

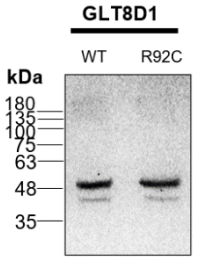

Figure 3.7- Immunoblotting of recombinant full-length GLT8D1-wt and GLT8D1-R92C from HEK293 cells. SDS-PAGE was performed in non-reducing conditions. Thirty μg protein were applied per lane. Molecular mass markers are indicated on the left. Detection was done using the Enhanced Chemiluminescence method.

GLT8D1 has three potential N-glycosylation sites at Asn-103, Asn-249 and Asn-257. To confirm that those sites were occupied proteins were incubated with PNGase F, which is an enzyme that removes N-glycans of the complex, hybrid and high mannose types from glycoproteins, and Endo-H which removes N-glycans of the high mannose and hybrid type. (section 2.6 Materials and Methods). There was a downward shift of GLT8D1-wt with both enzymes to bands with comparable masses (Figure 3.8). These results indicated that the protein was N-glycosylated, and the N-glycans were predominantly of the high mannose and hybrid types. The band at lower molecular mass in the control could consist of a non-glycosylated form.

The pattern of deglycosylation was similar for the wild-type and mutant forms, which indicated there were probably no major differences in N-glycosylation between the two forms.

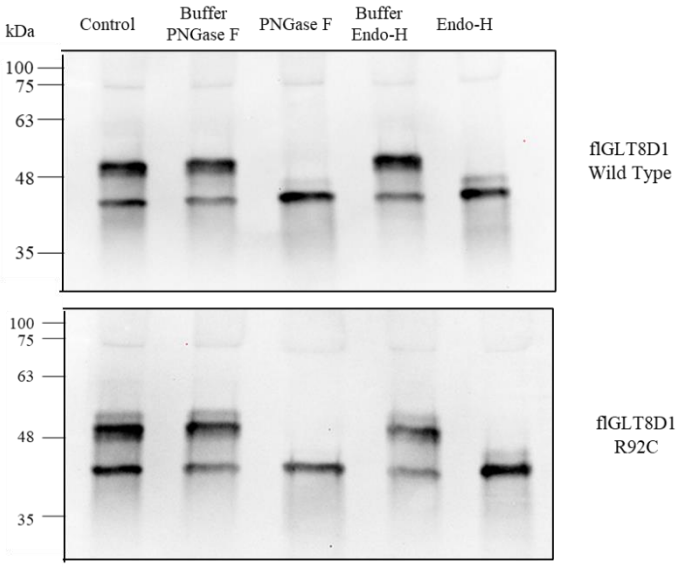

Figure 3.8- Immunoblotting of recombinant full-length GLT8D1, either wild type or R92C mutant, from HEK293 cells. Deglycosylation with peptide N-glycosidase F (PNGase F) and endoglycosidase H (Endo-H) is shown. GLT8D1 without treatment (Control), incubated without (Buffer) or with enzyme is indicated on top of the lanes. 0.55 µg protein in 15 µL were applied per lane. Molecular mass markers are indicated on the left. For detection, primary antibody Anti-FLAG M2 (dilution 1:4000) and secondary Sheep anti-mouse (dilution 1:4000) were used. Detection was done by using the Enhanced Chemiluminescence method.

The soluble secreted form of GLT8D1 (sGLT8D1, Figure 2.1 Materials and Methods) consisted of the catalytic domain of the enzyme with 8 fusion tags at the N-terminus. It migrated in SDS-PAGE between 63 and 75 kDa (Control lane in Figure 3.9).

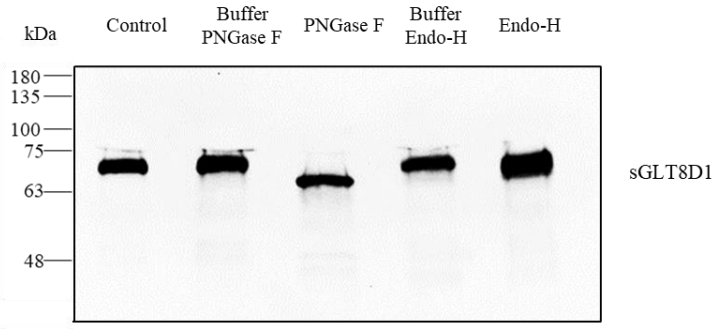

Figure 3.9- Immunoblotting of recombinant sGLT8D1 from HEK293 cells. Deglycosylation with peptide N-glycosidase F (PNGase F) and endoglycosidase H (Endo-H) is shown. The enzyme was not incubated (Control), or incubated without (Buffer) or with enzyme as indicated on top of the lanes. 200 ng of protein in 15 µL were applied per lane. Molecular mass markers are indicated on the left. For detection, primary antibody Anti-His Tag (dilution 1:7000) and secondary Sheep anti-mouse (dilution 1:3000) were used. Detection was done using the Enhanced Chemiluminescence method.

sGLT8D1 was incubated with Endo-H and PNGase F, which resulted in a downward shift in the apparent molecular mass (Figure 3.9), which indicated that the protein was N-glycosylated. The mass shift observed was higher when using PNGase F than when using Endo-H, which suggested that the N-glycosylation sites of the soluble protein were occupied by both high mannose/hybrid glycans as well as complex glycans.

3.2.2. Enzymatic activity of GLT8D1

3.2.2.1. Testing of the Universal Glycosyltransferase Activity Assay

GLT8D1 has been reported to be a galactosyltransferase [31], but the acceptor substrate was not known. Therefore, the Universal Glycosyltransferase Activity Assay from Promega has been used to test enzyme activity with UDP-Gal as the sugar nucleotide donor. In this assay the UDP released is proportional to the luminescence values in RLU, and, thus, provides a measure of the enzymatic galactosyltransferase activity.

In the first step, the assay has been implemented in the laboratory using well-studied galactosyltransferase (GalT) from human milk. GalT catalyzes the transfer of galactose from the donor substrate UDP-Gal to glucose with the production of lactose (Gal-Glc) [129] (Figure 3.10).

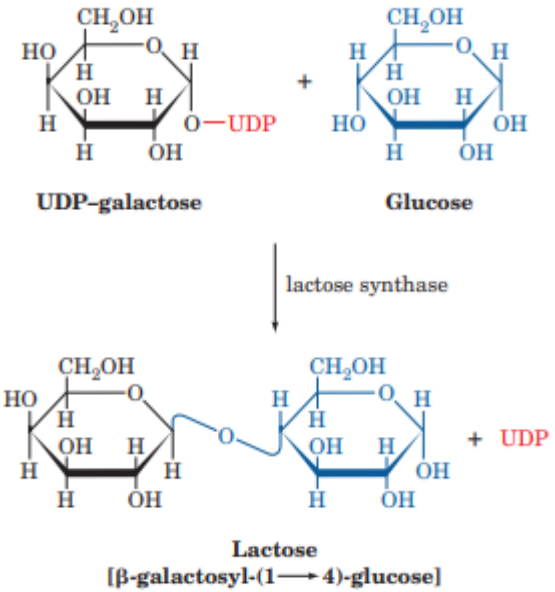

Figure 3.10- Reaction catalyzed by GalT from milk. This enzyme catalyzes the formation of lactose from UDP-Gal and Glc. Figure adapted from [129].

It is known that mammalian galactosyltransferase is activated by regulatory protein α-lactalbumin [130]. Therefore, GalT activity from milk was tested in the presence or absence of α-lactalbumin. Luminescence levels confirmed the synthesis of lactose by milk GalT in the presence of α-lactalbumin by using the Universal Glycosyltransferase Activity kit (Figure 3.11).

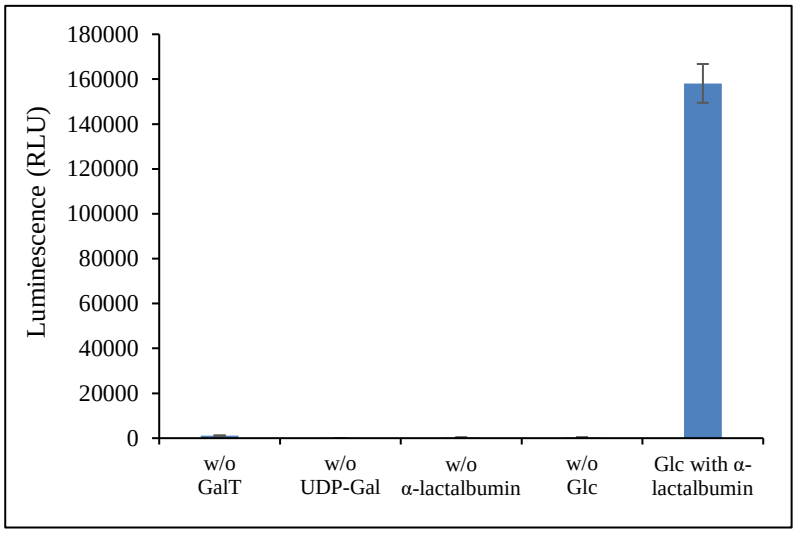

Figure 3.11- GalT activity from milk. Reaction mixture used in the assay was composed of 50 mM Tris HCl pH 7.5, 5 mM $MnCl_2$, 0.03 U/mL GalT, 0.2 mg/mL α-lactalbumin, 20 mM Glc, and 0.1 mM UDP-Gal. Incubation time was for 2 h at 37 °C. Data represents average of duplicates and error bars represent standard deviation.

3.2.2.2. Investigation of GLT8D1 acceptor substrates

The specificity of sGLT8D1 towards monosaccharides, small oligosaccharides and N-glycans was investigated using Universal Glycosyltransferase Activity assay. All used molecules with their respective structures are represented in Appendix 7.1.

Results from the screening of several monosaccharides is represented in Figure 3.12. The results showed that GlcNAc had higher signal when compared to the control without the enzyme and the other tested monosaccharides, presenting values slightly above 2500 RLU. Therefore, GlcNAc appeared as a substrate acceptor of sGLT8D1 *in vitro*. The expected reaction product would be the disaccharide N-acetyllactosamine (GlcNAc-Gal, LacNAc) (Figure 3.13). Since there was evidence of enzymatic activity using GlcNAc, the subquente studies were always compared to this acceptor.

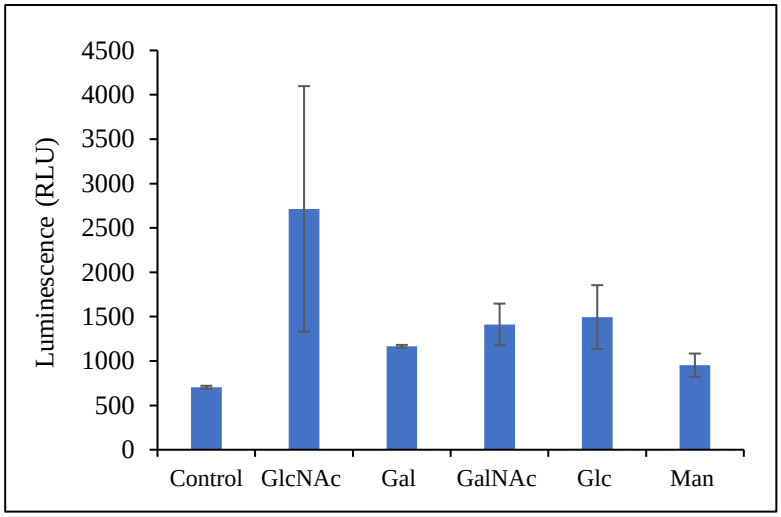

Figure 3.12- Monosaccharides screening as acceptors using GLT8D1. GLT8D1 protein was incubated for 16 h with 50 mM Tris HCl pH 7.5, 5 mM $MnCl_2$, 20 mM of each acceptor and 0.1 mM UDP-Gal. Data represents average of duplicates and error bars represent standard deviation.

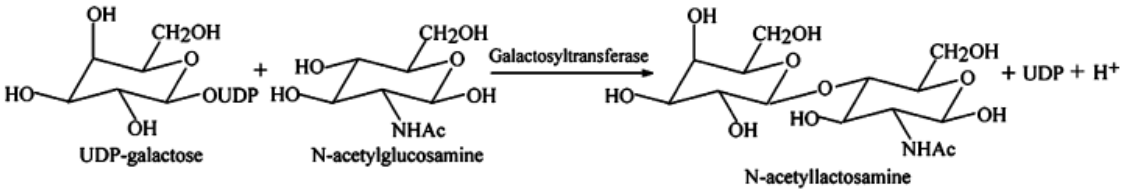

Figure 3.13- Reaction catalyzed by galactosyltransferase GLT8D1 using GlcNAc as acceptor molecule. Figure adapted from [130].

The effect of α-lactalbumin in GLT8D1 enzymatic activity was tested, in comparison to the previous results with milk GalT. However, α-lactalbumin did not constitute an activator of GLT8D1.

To confirm GlcNAc as sGLT8D1 acceptor a time course experiment was done up to 24 h incubation (Figure 3.14). The findings showed an increase over time of the RLU values, which supported the sGLT8D1 was capable of transferring Gal from UDP-Gal to GlcNAc. The lower increase in RLU with time in the absence of enzyme probably corresponded to spontaneous hydrolysis activity of UDP-Gal.

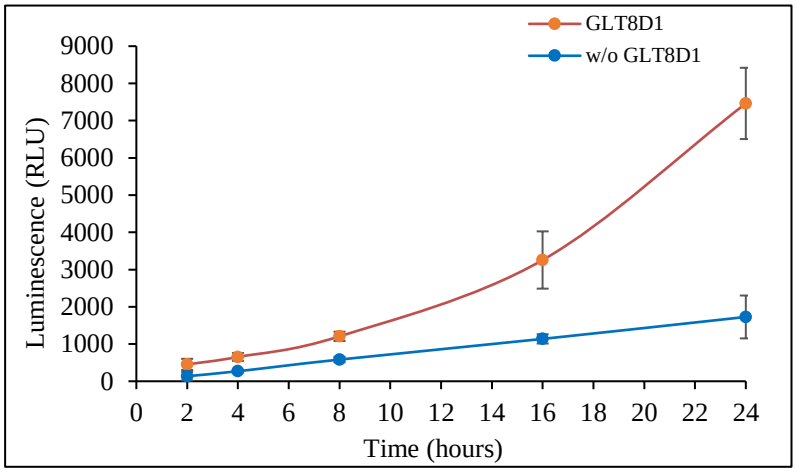

Figure 3.14- Time course of sGLT8D1 activity.
sGLT8D1 concentration was 0.017 mg/mL. Incubation buffer consisted of 50 mM Tris HCl pH 7.5, 5 mM MnCl2, 0.5 mM UDP-Gal and 20 mM GlcNAc. Data was performed in triplicates and error bars represent standard deviation.

Then, several small oligosaccharides were tested as potential acceptors of sGLT8D1 and GlcNAc was used as positive control (Figure 3.15). For all the oligosaccharides tested there was no detectable enzyme activity since the RLU levels were comparable in the presence or absence of enzyme, which indicated that they did not constitute sGLT8D1 acceptors *in vitro*.

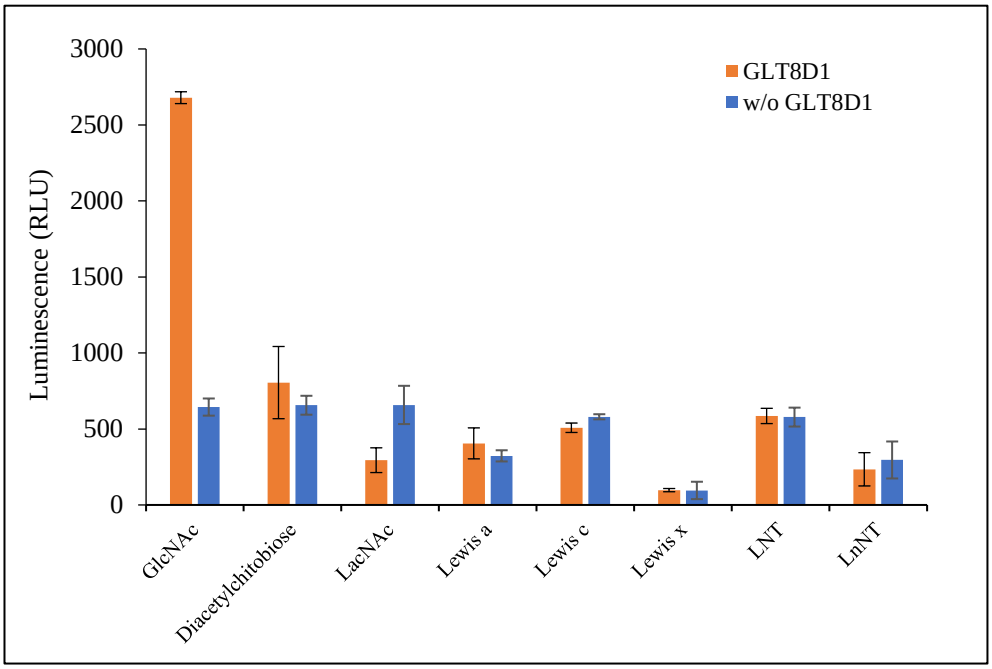

Figure 3.15- sGLT8D1 activity towards small oligosaccharides.
Results correspond to incubations with (orange bars) and without (blue bars) enzyme. Incubations were in 50 mM Tris HCl pH 7.5, 5 mM $MnCl_2$ and 0.1 mM UDP-Gal for 16 h. Acceptors final concentration is specified in Appendix 7.1. Data represents average of duplicates and error bars represent standard deviation.

Since GlcNAc is present in N-glycans activity of sGLT8D1, activity towards complex N-glycans was investigated (Figure 3.16). Results showed high RLU levels when using FA2B and A2B acceptors but not with the remaining compounds. However, the RLU level was also high in the incubation without the enzyme.

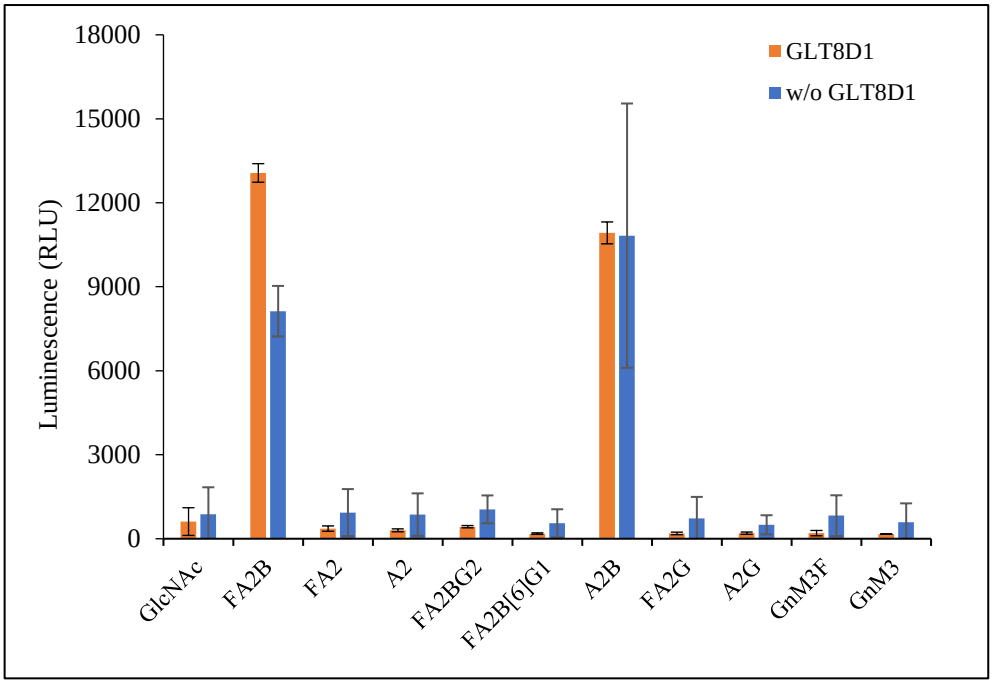

Figure 3.16- sGLT8D1 activity towads N-glycans.
Results corresponded to incubations with (orange bars) or without (blue bars) enzyme. Incubations were of 16 h with 50 mM Tris HCl pH 7.5, 5 mM $MnCl_2$ and 0.2 mM UDP-Gal. Acceptors final concentration is specified in Appendix 7.1. Data represents average of duplicates and error bars represent standard deviation.

This could be due to hydrolysis of UDP-Gal or to the presence of some contaminant in these assays that would interfere with the Universal Glycosyltransferase Activity assay. Since this assay was only performed on one occasion it will be necessary to repeat it and clarify the significance of these findings.

3.2.3. UHPLC-MS for confirmation of acceptor

sGLT8D1 was found to transfer Gal from UDP-Gal to GlcNAc, and the expected reaction product would be LacNAc. To investigate this hypothesis, the reaction mixture after 16 h incubation was analysed by NMR, but LacNAc was not detected possibly due to the low amount of product combined with the low sensitivity of the technique (Appendix 7.2).
Then, the reaction mixture after incubation was passed through a HyperCarb cartridge to purify any present oligosaccharides (including putative LacNAc), and these were analysed by UHPLC-MS/MS in parallel with LacNAc standard of commercial origin. The separation was with a Thermo Hypercarb column and data was acquired on a Q Exactive Focus. A signal with *m/z*

384.15 eluting at retention time 5.3 minutes was found, which was comparable to that of standard LacNAc. This result supported the presence of LacNAc.

For more accurate confirmation the MS^2 fragmentation pattern of standard LacNAc was compared with that of LacNAc from mzCloud data base and a match of 96.3 % was found (Figure 3.17A). The same approach was done for the sGLT8D1 reaction product, and a 95.5 % match was found (Figure 3.17B). These results demonstrated that sGLT8D1 catalyzed the production of LacNAc.

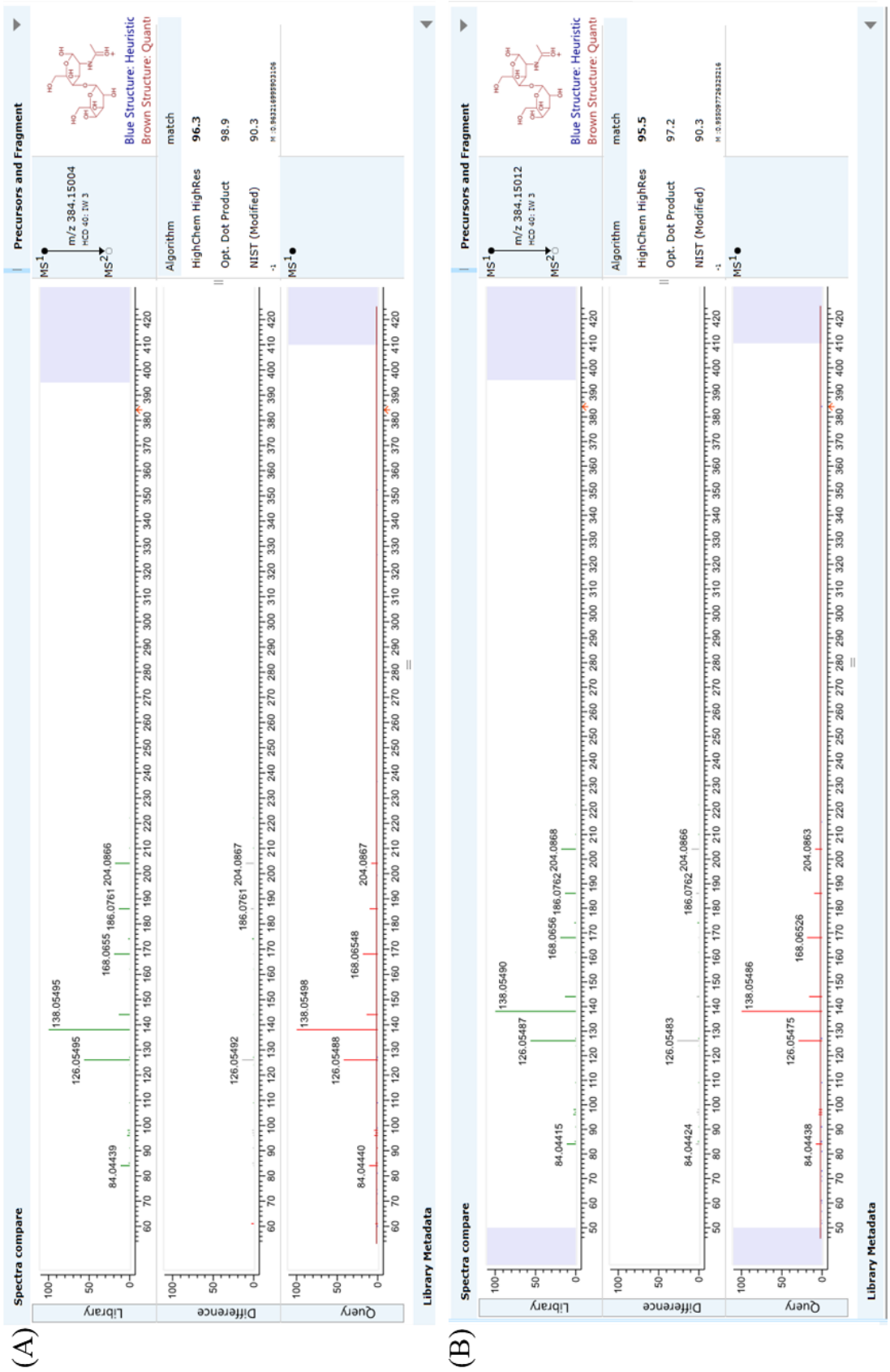

Figure 3.17- MS^2 spectra of LacNAc.
(A) MS^2 spectra of standard LacNAc and **(B)** disaccharide reaction product of sGLT8D1 were compared with MS^2 spectrum of LacNAc from mzCloud data base. Results were obtained by at UniMS, ITQB NOVA (Conceição Almeida, Catarina Correia, Dr. Ana Guerreiro).

4. Discussion

In this thesis, proteins associated with mechanisms of pathogenesis in ALS have been studied. First, CHIT1 a protein related with neuroinflammation has been quantified from the plasma of ALS patients using a newly implemented ELISA assay and compared with healthy controls to evaluate its biomarker potential. Secondly, GLT8D1, a glycosylated glycosyltransferase that was recently found mutated in families with ALS, has been characterized, particularly regarding the elucidation of its specificity *in vitro*.

4.1. Plasma CHIT1

Aiming at plasma CHIT1 a sandwich ELISA assay has been implemented in the laboratory. Although there are commercially available kits for CHIT1 quantification they are very expensive, therefore the assay developed here presented the advantage of lower cost, easier availability and higher versatility since it could be adapted to test CHIT1 from complex mixtures such as plasma. Testing combinations of different antibody concentrations, one blocking condition, washing buffer and time, allowed to obtain a robust assay for quantitative purposes with calibration curves with high correlation coefficients. Furthermore, spike controls showed that it was suitable for CHIT1 quantification from the plasma. The lowest concentration detected in the calibration curve was 56.25 pg/mL. Plasma needed to be diluted 1:50 or 1:75 fold to determine CHIT1 concentration by interpolation in the calibration curve.

Concentration values obtained for plasma CHIT1 were within the range described in earlier reports [123,124,126].

Although extensive, most studies regarding the potential of CHIT1 as an ALS biomarker, relied on CSF, with very few addressing this potential biomarker in blood. In CSF, CHIT1 is found significantly higher in ALS patients compared to both healthy and disease controls according to several reports [111,120,121,125]. Furthermore, correlations with several parameters were also established, such as correlation between CSF CHIT1 levels and PR with a $p<0.001$ [111,120,125].

Blood (plasma or serum) collection is less invasive for the patient and, therefore, more accessible for biomarker testing. Previous studies concerning CHIT1 levels in the blood of ALS patients are contradictory. On one hand, CHIT1 activity was found to be higher in dry blood of patients with ALS [126]. On the other hand, other authors found trends towards an increase in ALS but not significant [123–125]. In another study, a significant increase was found only for one cohort of genetic ALS patients from two cohorts investigated [127]. In this study, a trend towards an increase in CHIT1 levels has been found for ALS patients with a suboptimal diagnostic performance AUC=0.67 (p=0.080). This value was slightly higher than the reported by others

regarding plasma CHIT1 (AUC=0.60) [125]. The difference observed by different groups might be due to the diversity of analysed populations.

Some patients had extremely low levels of CHIT1 that were classified as outliers. These patients may have a common duplication in exon 10 of *CHIT1* gene that leads to reduced expression and activity [94,111].

Potential correlations of plasma CHIT1 levels with demographic and clinical parameters were also investigated but there was no correlation found with any of the scored parameters, age at sampling, age at onset, years with disease, ALSFRS and respiratory subscore, disease progression, the respiratory function index forced vital capacity (FVC), pCO_2 or sPO_2. In agreement with these results, a recent study did not find differences in plasma CHIT1 levels among fast, intermediate, slow progressors, ALSFRS-R or disease duration either [125]. In contrast, concerning FVC, which measures potential respiratory impairment in ALS, a significant correlation was found with plasma CHIT1 [126]. According to a research in 2006 [131], the value of FVC may constitute a predictor for survival and disease progression.

The results of CHIT1 levels from the plasma appear less promising biomarkers than CHIT1 from the CSF. Particularly, CSF CHIT1 had significant correlation with progression rate confirmed in independent studies [121,123,124] and fast progressors had higher levels of CHIT1 than slow progressors [125]. Furthermore, CSF CHIT1 was also found to correlate moderately with ALSFRS-R [124]. Additionally, a significant negative correlation between CSF CHIT1 and FVC has recently been reported [121].

Elevated levels of CHIT1 in the CSF are indicative of glial activation associated with neuroinflammation resulting from motor neuron damage in ALS [124]. On the other hand, CHIT1 from plasma is mainly secreted by activated macrophages but it is possible that some CHIT1 from neuronal tissue is transferred to peripheral blood of patients through the blood-brain barrier, representing part of the detected values. However, the difference between the biomarker potential of CSF CHIT1 (from literature) and plasma CHIT1 (obtained in this study), probably suggests that different and potentially independent mechanisms drive changes of CHIT1 levels in CSF and blood and the transfer across the blood-brain barrier is not extensive. Alternatively, the slightly increased levels of CHIT1 in peripheral blood of ALS patients may also indicate that patients may have peripheral signs of inflammation [127]. In agreement, changes in systemic inflammatory markers have been reported in the blood of ALS patients [78].

4.2. GLT8D1

GLT8D1 started to be investigated more recently in the context of ALS since mutations have been found in the enzyme in some cases of familial ALS. In the mutant form flGLT8D1-R92C an arginine residue was replaced by a cysteine residue in the 92 position, and cysteine residues may potentially form disulfide bonds. However, in this study, immunoblotting analysis under non-reducing conditions showed that the mutant form did not form dimers or oligomers that would be mediated by the newly introduced cysteine since both the wild-type and the mutant form had a mass of around 48 kDa. When proteins oligomerize, their size and molecular weight increases in discrete increments corresponding to the addition of separate proteins. Nevertheless, the introduced mutation could induce changes in conformation of the protein that would affect its activity and function. Potential changes could be investigated by biophysical and structural analysis techniques, such as circular dichroism or X-ray crystallography.

flGLT8D1-wt has three potential N-glycosylation sites. In this study the glycosylation patterns of flGLT8D1-wt, flGLT8D1-R92C and sGLT8D1 were investigated using two deglycosylation enzymes, Endo-H that cleaves high mannose and hybrid glycans and PNGase F that cleaves high mannose, hybrid and complex glycans. The results showed that flGLT8D1-wt and flGLT8D1-R92C were deglycosylated with the two enzymes with a comparable downward shift in SDS-PAGE. This result indicated that both the wild-type and the mutant form were N-glycosylated with high mannose/hybrid type glycans. On the other hand, sGLT8D1 protein had a larger mass decrease when digested with PNGase F than with Endo-H. These findings indicated that sGLT8D1 had both high mannose and complex type glycans in its structure.

flGLT8D1 is a type II transmembrane protein mainly detected in the Golgi apparatus [31], while sGLT8D1 is the secreted form of the protein containing the catalytic domain. The assembly of N-glycans follows a sequence of events from endoplasmic reticulum to the Golgi apparatus. The modifications of N-glycans in the Golgi contribute to the formation of variably branched and extended structures present in glycoproteins. The different N-glycans present in either the full-length membrane bound protein, or the secreted protein could be the result of a higher accessibility of the N-glycan processing machinery to the latter form. Therefore, some of the N-glycans present in sGLT8D1 were more extensively processed thus becoming complex structures.

The results showing that GLT8D1 was N-glycosylated were in agreement with previous findings where human glycosyltransferases were reported to be N-glycosylated [42]. Those N-glycans may be important for their proper folding involving the calnexin cycle in the endoplasmic reticulum as previously reported for fucosyltransferase 3 [39], and may also contribute to their stability by preventing proteolytic degradation.

Through sequence homology GLT8D1 was classified as a member of glycosyltransferase family 8 that catalyzes the transfer of a glycosyl group from a donor to an acceptor (CAZy database; http://www.cazy.org/). In a theoretical work GLT8D1 has been predicted to have glucosyltransferase activity [46]. However, using a practical approach another group showed that GLT8D1 used UDP-Gal as sugar nucleotide substrate with the UDP-Glo™ Glycosyltransferase assay from Promega [31], therefore, suggesting that it would be a galactosyltransferase. However, the potential acceptor was not identified.

In this study, the acceptor specificity for GLT8D1 has been investigated also using the UDP-Glo™ Glycosyltransferase assay from Promega. Several monosaccharides, small oligosaccharides and N-glycans were investigated as potential acceptors using UDP-Gal as the donor. The results indicated that N-acetylglucosamine (GlcNAc) was an acceptor of GLT8D1 activity and confirmed that GLT8D1 had galactosyltransferase activity. The expected reaction product would be N-acetyllactosamine (LacNAc).

The Promega assay is based on UDP release from the reaction, so it was necessary to confirm the formation of LacNAc by detailed structural analysis, which was accomplished by using LC-MS/MS. In fact, a compound at m/z 384.15 was detected that had a MS^2 fragmentation pattern with a high match (95.5%) in comparison to that of LacNAc. These results confirmed that GLT8D1 synthesized LacNAc *in vitro*.

The efficiency of Gal transfer was low, therefore more complex molecules containing GlcNAc including small oligosaccharides and N-glycans were tested as potential acceptors. Amongst the tested ones, only two complex N-glycans, diantennary minus two Gal plus 1 bisecting GlcNAc plus proximal Fuc (FA2B) and diantennary minus two Gal plus bisecting GlcNAc (A2B) showed significant high signals of GLT8D1 enzymatic activity using the Promega assay. Both FA2B and A2B contain three available GlcNAc residues that could constitute potential GLT8D1 acceptors (Appendix 7.1). However, the preliminary results showed that there was UDP release even in the absence of the enzyme. These results need to be further investigated.

This work opened novel perspectives to explore biological macromolecules (glycolipids, glycoproteins, proteoglycans) containing GlcNAc that would constitute endogenous cellular substrates of GLT8D1. Such molecules could participate in important cellular events such as signaling, and provide information about the function of the enzyme and its implications in neurodegeneration. Another relevant aspect is the potential use of GLT8D1 for the *in vitro* synthesis of galactosylated glycoconjugates, once more efficient substrates have been identified.

GLT8D1 is a protein with impact in ALS since the mutants detected in ALS induced cytotoxicity in HEK293 and N2A cells, and caused motor problems in zebrafish consistent with ALS [31]. On the other hand, a genetic correlation between the gene *GLT8D1* and schizophrenia

[35,38] as well as other psychiatric disorders [38] has been found. Curiously, a genetic correlation between ALS and schizophrenia has recently been described [36]. GLT8D1 was found to play a role in neuron differentiation from neural stem cells as well as in morphology and synaptic transmission of differentiated neurons [35]. On the other hand, GLT8D1 was recently proposed as prognostic marker for melanoma [37]. Therefore, the elucidation of the enzymatic properties and function of GLT8D1 will be relevant not only in ALS but also in other diseases.

5. Conclusions and future perspectives

In this work a sandwich ELISA assay has been implemented that allowed plasma CHIT1 quantification and may also be used for quantification of the protein in other biofluids and supernatants of disease cell models in culture.

Quantifications in this study indicated that CHIT1 from plasma samples does not have a promising potential as biomarker for ALS regarding diagnosis, progression rate or FVC, in contrast to that reported in the literature for CHIT1 from the CSF.

Regarding protein GLT8D1, this study showed that full-length wild-type and mutant R92C as well as secreted enzyme were N-glycosylated. Membrane bound and soluble forms had different glycosylation types as evaluated by sensitivity to digestion with Endo-H and PNGase F. Future studies concerning this matter could address detailed structure analysis of the N-glycans or mutation of the glycosylation sites to investigate glycans function in GLT8D1. In addition, it would be relevant to further investigate possible finer changes in glycosylation caused by the R92C mutation.

Finally, it was demonstrated that GLT8D1 has galactosyltransferase activity using UDP-Gal as sugar nucleotide donor and GlcNAc as acceptor, with the synthesis of LacNAc *in vitro*. This result opens novel perspectives to investigate GlcNAc carrier molecules as potentially more efficient acceptors. Those will provide a basis to clarify the biological function of this less studied glycosyltransferase and its impact in ALS as well as psychiatric diseases such as schizophrenia. In view of the obtained results, applications of GLT8D1 for the *in vitro* synthesis of bioactive glycoconjugates are also a possibility.

6. References

1. Rowland LP. How Amyotrophic Lateral Sclerosis Got Its Name. *Arch Neurol*. 2001;58(3):512-515. doi:10.1001/archneur.58.3.512

2. Brooks BR. El escorial World Federation of Neurology criteria for the diagnosis of amyotrophic lateral sclerosis. *J Neurol Sci*. 1994;124(SUPPL.):96-107. doi:10.1016/0022-510X(94)90191-0

3. Brooks BR, Miller RG, Swash M, Munsat TL. El Escorial revisited: Revised criteria for the diagnosis of amyotrophic lateral sclerosis. *Amyotroph Lateral Scler*. 2000;1(5):293-299. doi:10.1080/146608200300079536

4. Andersen PM. Amyotrophic lateral sclerosis associated with mutations in the CuZn superoxide dismutase gene. *Curr Neurol Neurosci Rep*. 2006;6(1):37-46. doi:10.1007/s11910-996-0008-9

5. Yeo CJJ, Simmons Z. Discussing edaravone with the ALS patient: an ethical framework from a U.S. perspective. *Amyotroph Lateral Scler Front Degener*. 2018;19(3-4):167-172. doi:10.1080/21678421.2018.1425455

6. Cedarbaum JM. The amyotrophic lateral sclerosis functional rating scale: Assessment of activities of daily living in patients with amyotrophic lateral sclerosis. *Arch Neurol*. 1996;53(2):141-147. doi:10.1001/archneur.1996.00550020045014

7. Cedarbaum JM, Stambler N, Malta E, et al. The ALSFRS-R: a revised ALS functional rating scale that incorporates assessments of respiratory function. *J Neurol Sci*. 1999;169(1-2):13-21. doi:10.1016/S0022-510X(99)00210-5

8. Abe K, Aoki M, Tsuji S, et al. Safety and efficacy of edaravone in well defined patients with amyotrophic lateral sclerosis: a randomised, double-blind, placebo-controlled trial. *Lancet Neurol*. 2017;16(7):505-512. doi:10.1016/S1474-4422(17)30115-1

9. Masrori P, Van Damme P. Amyotrophic lateral sclerosis: a clinical review. *Eur J Neurol*. 2020;27(10):1918-1929. doi:10.1111/ene.14393

10. Logroscino G, Piccininni M. Amyotrophic lateral sclerosis descriptive epidemiology: The origin of geographic difference. *Neuroepidemiology*. 2019;52(1-2):93-103. doi:10.1159/000493386

11. Logroscino G, Traynor BJ, Hardiman O, et al. Incidence of amyotrophic lateral sclerosis in Europe. *J Neurol Neurosurg Psychiatry*. 2010;81(4):385-390. doi:10.1136/jnnp.2009.183525

12. van Es MA, Hardiman O, Chio A, et al. Amyotrophic lateral sclerosis. *Lancet*. 2017;390(10107):2084-2098. doi:10.1016/S0140-6736(17)31287-4

13. Brown RH, Al-Chalabi A. Amyotrophic Lateral Sclerosis. Longo DL, ed. *N Engl J Med*. 2017;377(2):162-172. doi:10.1056/NEJMra1603471

14. Brotman RG, Moreno-Escobar MC, Joseph J, Pawar G. *Amyotrophic Lateral Sclerosis*. StatPearls Publishing; 2021. http://www.ncbi.nlm.nih.gov/pubmed/32310611. Accessed December 2, 2020.

15. La Spada A. *Spinal and Bulbar Muscular Atrophy*. University of Washington, Seattle; 1993. http://www.ncbi.nlm.nih.gov/pubmed/20301508. Accessed December 1, 2020.

16. Turner MR, Talbot K. Primary lateral sclerosis: Diagnosis and management. *Pract Neurol*. 2020;20(4):262-269. doi:10.1136/practneurol-2019-002300

17. Raaphorst J, Beeldman E, De Visser M, De Haan RJ, Schmand B. A systematic review of behavioural changes in motor neuron disease. *Amyotroph Lateral Scler*. 2012;13(6):493-501. doi:10.3109/17482968.2012.656652

18. Rowland LP. Progressive muscular atrophy and other lower motor neuron syndromes of adults. *Muscle Nerve*. 2010;41(2):161-165. doi:10.1002/mus.21565

19. Mejzini R, Flynn LL, Pitout IL, Fletcher S, Wilton SD, Akkari PA. ALS Genetics, Mechanisms, and Therapeutics: Where Are We Now? *Front Neurosci*. 2019;13(December):1-27. doi:10.3389/fnins.2019.01310

20. Rosen DR, Siddique T, Patterson D, et al. Mutations in Cu/Zn superoxide dismutase gene are associated with familial amyotrophic lateral sclerosis. *Nature*. 1993;362(6415):59-62. doi:10.1038/362059a0

21. Hadano S, Hand CK, Osuga H, et al. A gene encoding a putative GTPase regulator is mutated in familial amyotrophic lateral sclerosis 2. *Nat Genet*. 2001;29(2):166-173. doi:10.1038/ng1001-166

22. Sreedharan J, Blair IP, Tripathi VB, et al. TDP-43 Mutations in Familial and Sporadic Amyotrophic Lateral Sclerosis. *Science (80-)*. 2008;319(5870):1668-1672. doi:10.1126/science.1154584

23. Maruyama H, Morino H, Ito H, et al. Mutations of optineurin in amyotrophic lateral sclerosis. *Nature*. 2010;465(7295):223-226. doi:10.1038/nature08971

24. Deng HX, Chen W, Hong ST, et al. Mutations in UBQLN2 cause dominant X-linked juvenile and adult-onset ALS and ALS/dementia. *Nature*. 2011;477(7363):211-215. doi:10.1038/nature10353

25. DeJesus-Hernandez M, Mackenzie IR, Boeve BF, et al. Expanded GGGGCC Hexanucleotide Repeat in Noncoding Region of C9ORF72 Causes Chromosome 9p-Linked FTD and ALS. *Neuron*. 2011;72(2):245-256. doi:10.1016/j.neuron.2011.09.011

26. Vance C, Lehmann R, Broihier HT, et al. Mutations in FUS, an RNA processing protein, cause familial amyotrophic lateral sclerosis type 6. *Science (80-)*. 2009;323(February):1208-1211. doi:10.1126/science.1165942.Mutations

27. Freischmidt A, Wieland T, Richter B, et al. Haploinsufficiency of TBK1 causes familial ALS and fronto-temporal dementia. *Nat Neurosci*. 2015;18(5):631-636. doi:10.1038/nn.4000

28. Brenner D, Yilmaz R, Müller K, et al. Hot-spot KIF5A mutations cause familial ALS. *Brain*. 2018;141(3):688-697. doi:10.1093/brain/awx370

29. Mackenzie IR, Nicholson AM, Sarkar M, et al. TIA1 Mutations in Amyotrophic Lateral Sclerosis and Frontotemporal Dementia Promote Phase Separation and Alter Stress Granule Dynamics. *Neuron*. 2017;95(4):808-816.e9. doi:10.1016/j.neuron.2017.07.025

30. Topp SD, Fallini C, Shibata H, et al. Mutations in the vesicular trafficking protein Annexin A11 are associated with amyotrophic lateral sclerosis Bradley N. Smith. *Sci Transl Med*. 2017;9(388):1-16. doi:10.1126/scitranslmed.aad9157

31. Cooper-Knock J, Moll T, Ramesh T, et al. Mutations in the Glycosyltransferase Domain of GLT8D1 Are Associated with Familial Amyotrophic Lateral Sclerosis. *Cell Rep*. 2019;26(9):2298-2306.e5. doi:10.1016/j.celrep.2019.02.006

32. Zufiría M, Gil-Bea FJ, Fernández-Torrón R, et al. ALS: A bucket of genes, environment, metabolism and unknown ingredients. *Prog Neurobiol*. 2016;142:104-129. doi:10.1016/j.pneurobio.2016.05.004

33. Riancho J, Bosque-Varela P, Perez-Pereda S, Povedano M, de Munaín AL, Santurtun A. The increasing importance of environmental conditions in amyotrophic lateral sclerosis. *Int J Biometeorol*. 2018;62(8):1361-1374. doi:10.1007/s00484-018-1550-2

34. Yousefian-Jazi A, Seol Y, Kim J, Ryu HL, Lee J, Ryu H. Pathogenic Genome Signatures That Damage Motor Neurons in Amyotrophic Lateral Sclerosis. *Cells*. 2020;9(12):2687. doi:10.3390/cells9122687

35. Yang C-P, Li X, Wu Y, et al. Comprehensive integrative analyses identify GLT8D1 and CSNK2B as schizophrenia risk genes. *Nat Commun*. 2018;9(1):838. doi:10.1038/s41467-018-03247-3

36. McLaughlin RL, Schijven D, van Rheenen W, et al. Genetic correlation between amyotrophic lateral sclerosis and schizophrenia. *Nat Commun*. 2017;8(1):14774. doi:10.1038/ncomms14774

37. Hu H, Li Z, Zhou Y, et al. GLT8D1 overexpression as a novel prognostic biomarker in human cutaneous melanoma. *Melanoma Res*. 2019;29(6):612-620. doi:10.1097/CMR.0000000000000631

38. Wu Y, Cao H, Baranova A, et al. Multi-trait analysis for genome-wide association study of five psychiatric disorders. *Transl Psychiatry*. 2020;10(1):209. doi:10.1038/s41398-020-00902-6

39. Morais VA, Costa MT, Costa J. N-glycosylation of recombinant human fucosyltransferase III is required for its in vivo folding in mammalian and insect cells. *Biochim Biophys Acta - Gen Subj*. 2003;1619(2):133-138. doi:10.1016/S0304-4165(02)00448-8

40. Moll T, Shaw PJ, Cooper-Knock J. Disrupted glycosylation of lipids and proteins is a cause of neurodegeneration. *Brain*. 2020;143(5):1332-1340. doi:10.1093/brain/awz358

41. Barone R, Sturiale L, Palmigiano A, Zappia M, Garozzo D. Glycomics of pediatric and adulthood diseases of the central nervous system. *J Proteomics*. 2012;75(17):5123-5139. doi:10.1016/j.jprot.2012.07.007

42. Mikolajczyk K, Kaczmarek R, Czerwinski M. How glycosylation affects glycosylation: the role of N-glycans in glycosyltransferase activity. *Glycobiology*. 2020;30(12):941-969. doi:10.1093/glycob/cwaa041

43. Schneider JS. Altered expression of genes involved in ganglioside biosynthesis in substantia nigra neurons in Parkinson's disease. Dunbar GL, ed. *PLoS One*. 2018;13(6):e0199189. doi:10.1371/journal.pone.0199189

44. Lüdemann N, Clement A, Hans VH, Leschik J, Behl C, Brandt R. O-Glycosylation of the Tail Domain of Neurofilament Protein M in Human Neurons and in Spinal Cord Tissue of a Rat Model of Amyotrophic Lateral Sclerosis (ALS). *J Biol Chem*. 2005;280(36):31648-31658. doi:10.1074/jbc.M504395200

45. Desplats PA, Denny CA, Kass KE, et al. Glycolipid and ganglioside metabolism imbalances in Huntington's disease. *Neurobiol Dis*. 2007;27(3):265-277. doi:10.1016/j.nbd.2007.05.003

46. Taujale R, Venkat A, Huang L-C, et al. Deep evolutionary analysis reveals the design principles of fold A glycosyltransferases. *Elife*. 2020;9. doi:10.7554/eLife.54532

47. Li W, Liu Z, Sun W, et al. Mutation analysis of GLT8D1 and ARPP21 genes in amyotrophic lateral sclerosis patients from mainland China. *Neurobiol Aging*. 2020;85:156.e1-156.e4. doi:10.1016/j.neurobiolaging.2019.09.013

48. Costa J, Swash M, de Carvalho M. Awaji Criteria for the Diagnosis of Amyotrophic Lateral Sclerosis. *Arch Neurol*. 2012;69(11):1410. doi:10.1001/archneurol.2012.254

49. Taylor JP, Brown RH, Cleveland DW. Decoding ALS: from genes to mechanism. *Nature*. 2016;539(7628):197-206. doi:10.1038/nature20413

50. Pedersen JT, Heegaard NHH. Analysis of protein aggregation in neurodegenerative disease. *Anal Chem*. 2013;85(9):4215-4227. doi:10.1021/ac400023c

51. Neumann M, Sampathu DM, Kwong LK, et al. Ubiquitinated TDP-43 in Frontotemporal Lobar Degeneration and Amyotrophic Lateral Sclerosis. *Science (80-)*. 2006;314(5796):130-133. doi:10.1126/science.1134108

52. Okamoto K, Mizuno Y, Fujita Y. Bunina bodies in amyotrophic lateral sclerosis. *Neuropathology*. 2008;28(2):109-115. doi:10.1111/j.1440-1789.2007.00873.x

53. Wood JD, Beaujeux TP, Shaw PJ. Protein aggregation in motor neurone disorders. *Neuropathol Appl Neurobiol*. 2003;29(6):529-545. doi:10.1046/j.0305-1846.2003.00518.x

54. Harding HP, Calfon M, Urano F, Novoa I, Ron D. Transcriptional and translational control in the mammalian unfolded protein response. *Annu Rev Cell Dev Biol*. 2002;18:575-599. doi:10.1146/annurev.cellbio.18.011402.160624

55. Nussbacher JK, Tabet R, Yeo GW, Lagier-Tourenne C. Disruption of RNA Metabolism in Neurological Diseases and Emerging Therapeutic Interventions. *Neuron*. 2019;102(2):294-320. doi:10.1016/j.neuron.2019.03.014

56. Molliex A, Temirov J, Lee J, et al. Phase Separation by Low Complexity Domains Promotes Stress Granule Assembly and Drives Pathological Fibrillization. *Cell*. 2015;163(1):123-133. doi:10.1016/j.cell.2015.09.015

57. Majcher V, Goode A, James V, Layfield R. Autophagy receptor defects and ALS-FTLD. *Mol Cell Neurosci*. 2015;66(PA):43-52. doi:10.1016/j.mcn.2015.01.002

58. Nassif M, Woehlbier U, Manque PA. The Enigmatic Role of C9ORF72 in Autophagy. *Front Neurosci*. 2017;11(AUG):442. doi:10.3389/fnins.2017.00442

59. Ying H, Yue BYJT. Optineurin: The autophagy connection. *Exp Eye Res*. 2016;144:73-80. doi:10.1016/j.exer.2015.06.029

60. Finley D. Recognition and Processing of Ubiquitin-Protein Conjugates by the Proteasome. *Annu Rev Biochem*. 2009;78(1):477-513. doi:10.1146/annurev.biochem.78.081507.101607

61. Costa J, de Carvalho M. Esclerose lateral amiotrófica. In: LIDEL, ed. *Neurociências*. 2017th ed. ; 2017:592-604.

62. Guo W, Stoklund Dittlau K, Van Den Bosch L. Axonal transport defects and neurodegeneration: Molecular mechanisms and therapeutic implications. *Semin Cell Dev Biol*. 2020;99:133-150. doi:10.1016/j.semcdb.2019.07.010

63. Puls I, Jonnakuty C, LaMonte BH, et al. Mutant dynactin in motor neuron disease. *Nat Genet*. 2003;33(4):455-456. doi:10.1038/ng1123

64. Alami NH, Smith RB, Carrasco MA, et al. Axonal Transport of TDP-43 mRNA Granules Is Impaired by ALS-Causing Mutations. *Neuron*. 2014;81(3):536-543. doi:10.1016/j.neuron.2013.12.018

65. Carter BJ, Anklesaria P, Choi S, Engelhardt JF. Redox modifier genes and pathways in amyotrophic lateral sclerosis. *Antioxidants Redox Signal*. 2009;11(7):1569-1586. doi:10.1089/ars.2008.2414

66. Shibata N, Nagai R, Uchida K, et al. Morphological evidence for lipid peroxidation and protein glycoxidation in spinal cords from sporadic amyotrophic lateral sclerosis patients. *Brain Res*. 2001;917(1):97-104. doi:10.1016/S0006-8993(01)02926-2

67. Beal MF, Ferrante RJ, Browne SE, Matthews RT, Kowall NW, Brown RH. Increased 3-nitrotyrosine in both sporadic and familial amyotrophic lateral sclerosis. *Ann Neurol*. 1997;42(4):644-654. doi:10.1002/ana.410420416

68. Harraz MM, Marden JJ, Zhou W, et al. SOD1 mutations disrupt redox-sensitive Rac regulation of NADPH oxidase in a familial ALS model. *J Clin Invest*. 2008;118(2):659-670. doi:10.1172/JCI34060

69. Howland DS, Liu J, She Y, et al. Focal loss of the glutamate transporter EAAT2 in a transgenic rat model of SOD1 mutant-mediated amyotrophic lateral sclerosis (ALS). *Proc Natl Acad Sci*. 2002;99(3):1604-1609. doi:10.1073/pnas.032539299

70. Orsini M, Oliveira AB, Nascimento OJM, et al. Amyotrophic lateral sclerosis: New perpectives and update. *Neurol Int*. 2015;7(2):39-47. doi:10.4081/ni.2015.5885

71. Sasaki S, Warita H, Murakami T, et al. Ultrastructural study of aggregates in the spinal cord of transgenic mice with a G93A mutant SOD1 gene. *Acta Neuropathol*. 2005;109(3):247-255. doi:10.1007/s00401-004-0939-7

72. Sasaki S, Iwata M. Mitochondrial Alterations in the Spinal Cord of Patients With Sporadic Amyotrophic Lateral Sclerosis. *J Neuropathol Exp Neurol*. 2007;66(1):10-16. doi:10.1097/nen.0b013e31802c396b

73. Corti S, Donadoni C, Ronchi D, et al. Amyotrophic lateral sclerosis linked to a novel SOD1 mutation with muscle mitochondrial dysfunction. *J Neurol Sci*. 2009;276(1-2):170-174. doi:10.1016/j.jns.2008.09.030

74. Goodall EF, Morrison KE. Amyotrophic lateral sclerosis (motor neuron disease): proposed mechanisms and pathways to treatment. *Expert Rev Mol Med*. 2006;8(11):1-22. doi:10.1017/S1462399406010854

75. Inoue H, Tsukita K, Iwasato T, et al. The crucial role of caspase-9 in the disease progression of a transgenic ALS mouse model. *EMBO J*. 2003;22(24):6665-6674. doi:10.1093/emboj/cdg634

76. Li M. Functional Role of Caspase-1 and Caspase-3 in an ALS Transgenic Mouse Model. *Science (80-)*. 2000;288(5464):335-339. doi:10.1126/science.288.5464.335

77. Boston-Howes W, Gibb SL, Williams EO, Pasinelli P, Brown RH, Trotti D. Caspase-3 Cleaves and Inactivates the Glutamate Transporter EAAT2. *J Biol Chem*. 2006;281(20):14076-14084. doi:10.1074/jbc.M600653200

78. McCauley ME, Baloh RH. Inflammation in ALS/FTD pathogenesis. *Acta Neuropathol*. 2019;137(5):715-730. doi:10.1007/s00401-018-1933-9

79. Ravits J, Appel S, Baloh RH, et al. Deciphering amyotrophic lateral sclerosis: What phenotype, neuropathology and genetics are telling us about pathogenesis. *Amyotroph Lateral Scler Front Degener*. 2013;14(sup1):5-18. doi:10.3109/21678421.2013.778548

80. Geloso MC, Corvino V, Marchese E, Serrano A, Michetti F, D'Ambrosi N. The dual role of microglia in ALS: Mechanisms and therapeutic approaches. *Front Aging Neurosci*. 2017;9(JUL):242. doi:10.3389/FNAGI.2017.00242/BIBTEX

81. Beers DR, Appel SH. Immune dysregulation in amyotrophic lateral sclerosis: mechanisms and emerging therapies. *Lancet Neurol*. 2019;18(2):211-220. doi:10.1016/S1474-4422(18)30394-6

82. Thonhoff JR, Beers DR, Zhao W, et al. Expanded autologous regulatory T-lymphocyte infusions in ALS. *Neurol - Neuroimmunol Neuroinflammation*. 2018;5(4):e465. doi:10.1212/NXI.0000000000000465

83. Sheean RK, McKay FC, Cretney E, et al. Association of Regulatory T-Cell Expansion With Progression of Amyotrophic Lateral Sclerosis. *JAMA Neurol*. 2018;75(6):681. doi:10.1001/jamaneurol.2018.0035

84. Patin F, Baranek T, Vourc'h P, et al. Combined Metabolomics and Transcriptomics Approaches to Assess the IL-6 Blockade as a Therapeutic of ALS: Deleterious Alteration of Lipid Metabolism. *Neurotherapeutics*. 2016;13(4):905-917. doi:10.1007/s13311-016-0461-3

85. ORourke JG, Bogdanik L, Yanez A, et al. C9orf72 is required for proper macrophage and microglial function in mice. *Science (80-)*. 2016;351(6279):1324-1329. doi:10.1126/science.aaf1064

86. Burberry A, Suzuki N, Wang JY, et al. Loss-of-function mutations in the C9ORF72 mouse ortholog cause fatal autoimmune disease. *Sci Transl Med*. 2016;8(347). doi:10.1126/scitranslmed.aaf6038

87. Lee Y, Morrison BM, Li Y, et al. Oligodendroglia metabolically support axons and contribute to neurodegeneration. *Nature*. 2012;487(7408):443-448. doi:10.1038/nature11314

88. Kang SH, Li Y, Fukaya M, et al. Degeneration and impaired regeneration of gray matter oligodendrocytes in amyotrophic lateral sclerosis. *Nat Neurosci*. 2013;16(5):571-579. doi:10.1038/nn.3357

89. Wang L, Gutmann DH, Roos RP. Astrocyte loss of mutant SOD1 delays ALS disease onset and progression in G85R transgenic mice. *Hum Mol Genet*. 2011;20(2):286-293. doi:10.1093/hmg/ddq463

90. Vahsen BF, Gray E, Thompson AG, et al. Non-neuronal cells in amyotrophic lateral

sclerosis — from pathogenesis to biomarkers. *Nat Rev Neurol*. 2021;17(6):333-348. doi:10.1038/s41582-021-00487-8

91. Ihara Y, Nobukuni K, Takata H, Hayabara T. Oxidative stress and metal content in blood and cerebrospinal fluid of amyotrophic lateral sclerosis patients with and without a Cu, Zn-superoxide dismutase mutation. *Neurol Res*. 2005;27(1):105-108. doi:10.1179/016164105X18430

92. Noto Y-I, Shibuya K, Sato Y, et al. Elevated CSF TDP-43 levels in amyotrophic lateral sclerosis: Specificity, sensitivity, and a possible prognostic value. *Amyotroph Lateral Scler*. 2011;12(2):140-143. doi:10.3109/17482968.2010.541263

93. Tohgi H, Abe T, Yamazaki K, Murata T, Ishizaki E, Isobe C. Remarkable increase in cerebrospinal fluid 3-nitrotyrosine in patients with sporadic amyotrophic lateral sclerosis. *Ann Neurol*. 1999;46(1):129-131. doi:10.1002/1531-8249(199907)46:1<129::aid-ana21>3.0.co;2-y

94. Costa J, de Carvalho M. Emerging molecular biomarker targets for amyotrophic lateral sclerosis. *Clin Chim Acta*. 2016;455:7-14. doi:10.1016/j.cca.2016.01.011

95. Riancho J, Gil-Bea F, Santurtun A, López de Munaín A. Amyotrophic lateral sclerosis: a complex syndrome that needs an integrated research approach. *Neural Regen Res*. 2019;14(2):193. doi:10.4103/1673-5374.244783

96. Khalil M, Teunissen CE, Otto M, et al. Neurofilaments as biomarkers in neurological disorders. *Nat Rev Neurol*. 2018;14(10):577-589. doi:10.1038/s41582-018-0058-z

97. Deisenhammer F, Egg R, Giovannoni G, et al. EFNS guidelines on disease-specific CSF investigations. *Eur J Neurol*. 2009;16(6):760-e163. doi:10.1111/j.1468-1331.2009.02595.x

98. Feneberg E, Oeckl P, Steinacker P, et al. Multicenter evaluation of neurofilaments in early symptom onset amyotrophic lateral sclerosis. *Neurology*. 2018;90(1):e22-e30. doi:10.1212/WNL.0000000000004761

99. Steinacker P, Feneberg E, Weishaupt J, et al. Neurofilaments in the diagnosis of motoneuron diseases: a prospective study on 455 patients. *J Neurol Neurosurg Psychiatry*. 2015;87(1):jnnp-2015-311387. doi:10.1136/jnnp-2015-311387

100. Oeckl P, Jardel C, Salachas F, et al. Multicenter validation of CSF neurofilaments as diagnostic biomarkers for ALS. *Amyotroph Lateral Scler Front Degener*. 2016;17(5-6):404-413. doi:10.3109/21678421.2016.1167913

101. Weydt P, Oeckl P, Huss A, et al. Neurofilament levels as biomarkers in asymptomatic and symptomatic familial amyotrophic lateral sclerosis. *Ann Neurol*. 2016;79(1):152-158. doi:10.1002/ana.24552

102. Gonçalves M, Tillack L, de Carvalho M, Pinto S, Conradt HS, Costa J. Phosphoneurofilament heavy chain and N-glycomics from the cerebrospinal fluid in amyotrophic lateral sclerosis. *Clin Chim Acta*. 2015;438:342-349. doi:10.1016/j.cca.2014.09.011

103. Halbgebauer S, Steinacker P, Verde F, et al. Comparison of CSF and serum neurofilament light and heavy chain as differential diagnostic biomarkers for ALS. *J Neurol Neurosurg Psychiatry*. August 2021:jnnp-2021-327129. doi:10.1136/jnnp-2021-327129

104. Gaiottino J, Norgren N, Dobson R, et al. Increased Neurofilament Light Chain Blood Levels in Neurodegenerative Neurological Diseases. Reindl M, ed. *PLoS One*. 2013;8(9):e75091. doi:10.1371/journal.pone.0075091

105. Piehl F, Kockum I, Khademi M, et al. Plasma neurofilament light chain levels in patients with MS switching from injectable therapies to fingolimod. *Mult Scler J*. 2018;24(8):1046-1054. doi:10.1177/1352458517715132

106. Kuhle J, Barro C, Disanto G, et al. Serum neurofilament light chain in early relapsing remitting MS is increased and correlates with CSF levels and with MRI measures of disease severity. *Mult Scler J*. 2016;22(12):1550-1559. doi:10.1177/1352458515623365

107. Disanto G, Barro C, Benkert P, et al. Serum Neurofilament light: A biomarker of neuronal damage in multiple sclerosis. *Ann Neurol*. 2017;81(6):857-870. doi:10.1002/ana.24954

108. Li S, Ren Y, Zhu W, Yang F, Zhang X, Huang X. Phosphorylated neurofilament heavy chain levels in paired plasma and CSF of amyotrophic lateral sclerosis. *J Neurol Sci*. 2016;367:269-274. doi:10.1016/j.jns.2016.05.062

109. De Schaepdryver M, Jeromin A, Gille B, et al. Comparison of elevated phosphorylated neurofilament heavy chains in serum and cerebrospinal fluid of patients with amyotrophic lateral sclerosis. *J Neurol Neurosurg Psychiatry*. 2018;89(4):367-373. doi:10.1136/jnnp-2017-316605

110. Gille B, De Schaepdryver M, Dedeene L, et al. Inflammatory markers in cerebrospinal fluid: independent prognostic biomarkers in amyotrophic lateral sclerosis? *J Neurol Neurosurg Psychiatry*. 2019;90(12):jnnp-2018-319586. doi:10.1136/jnnp-2018-319586

111. Thompson AG, Gray E, Thézénas M-L, et al. Cerebrospinal fluid macrophage biomarkers in amyotrophic lateral sclerosis. *Ann Neurol*. 2018;83(2):258-268. doi:10.1002/ana.25143

112. Gaur N, Perner C, Witte OW, Grosskreutz J. The Chitinases as Biomarkers for Amyotrophic Lateral Sclerosis: Signals From the CNS and Beyond. *Front Neurol*. 2020;11:377. doi:10.3389/fneur.2020.00377

113. Pinteac R, Montalban X, Comabella M. Chitinases and chitinase-like proteins as biomarkers in neurologic disorders. *Neurol - Neuroimmunol Neuroinflammation*. 2021;8(1):e921. doi:10.1212/NXI.0000000000000921

114. Rosa M, Malaguarnera G, Gregorio C, D'Amico F, Mazzarino MC, Malaguarnera L. Modulation of Chitotriosidase During Macrophage Differentiation. *Cell Biochem Biophys*. 2013;66(2):239-247. doi:10.1007/s12013-012-9471-x

115. Di Rosa M, De Gregorio C, Malaguarnera G, Tuttobene M, Biazzo F, Malaguarnera L. Evaluation of AMCase and CHIT-1 expression in monocyte macrophages lineage. *Mol Cell Biochem*. 2013;374(1-2):73-80. doi:10.1007/s11010-012-1506-5

116. Kanneganti M. Role of Chitotriosidase (Chitinase 1) Under Normal and Disease Conditions. *J Epithel Biol Pharmacol*. 2012;5(1):1-9. doi:10.2174/1875044301205010001

117. Di Rosa M, Tibullo D, Cambria D, et al. Chitotriosidase Expression during Monocyte-Derived Dendritic Cells Differentiation and Maturation. *Inflammation*. 2015;38(6):2082-2091. doi:10.1007/s10753-015-0190-5

118. Fuchs K, Cardona Gloria Y, Wolz O-O, et al. The fungal ligand chitin directly binds TLR2 and triggers inflammation dependent on oligomer size. *EMBO Rep*. 2018;19(12). doi:10.15252/embr.201846065

119. Swash M. Chitinases, neuroinflammation and biomarkers in ALS. *J Neurol Neurosurg Psychiatry*. 2020;91(4):338-338. doi:10.1136/jnnp-2019-322520

120. Steinacker P, Feneberg E, Halbgebauer S, et al. Chitotriosidase as biomarker for early stage amyotrophic lateral sclerosis: a multicenter study. *Amyotroph Lateral Scler Front Degener*. 2021;0(0):1-11. doi:10.1080/21678421.2020.1861023

121. Costa J, Gromicho M, Pronto-Laborinho A, et al. Cerebrospinal Fluid Chitinases as Biomarkers for Amyotrophic Lateral Sclerosis. *Diagnostics*. 2021;11(7):1210. doi:10.3390/diagnostics11071210

122. Varghese AM, Sharma A, Mishra P, et al. Chitotriosidase - A putative biomarker for sporadic amyotrophic lateral sclerosis. *Clin Proteomics*. 2013;10(1):19. doi:10.1186/1559-0275-10-19

123. Thompson AG, Gray E, Bampton A, Raciborska D, Talbot K, Turner MR. CSF chitinase proteins in amyotrophic lateral sclerosis. *J Neurol Neurosurg Psychiatry*. 2019;90(11):1215-1220. doi:10.1136/jnnp-2019-320442

124. Steinacker P, Verde F, Fang L, et al. Chitotriosidase (CHIT1) is increased in microglia and macrophages in spinal cord of amyotrophic lateral sclerosis and cerebrospinal fluid levels correlate with disease severity and progression. *J Neurol Neurosurg Psychiatry*. 2017;89(3):239-247. doi:10.1136/jnnp-2017-317138

125. Vu L, An J, Kovalik T, Gendron T, Petrucelli L, Bowser R. Cross-sectional and longitudinal measures of chitinase proteins in amyotrophic lateral sclerosis and expression of CHI3L1 in activated astrocytes. *J Neurol Neurosurg Psychiatry*. 2019;91(4):350-358. doi:10.1136/jnnp-2019-321916

126. Pagliardini V, Pagliardini S, Corrado L, et al. Chitotriosidase and lysosomal enzymes as potential biomarkers of disease progression in amyotrophic lateral sclerosis: A survey clinic-based study. *J Neurol Sci*. 2015;348(1-2):245-250. doi:10.1016/j.jns.2014.12.016

127. Oeckl P, Weydt P, Steinacker P, et al. Different neuroinflammatory profile in amyotrophic lateral sclerosis and frontotemporal dementia is linked to the clinical phase. *J Neurol Neurosurg Psychiatry*. 2018;90(1):4-10. doi:10.1136/jnnp-2018-318868

128. Moremen KW, Ramiah A, Stuart M, et al. Expression system for structural and functional studies of human glycosylation enzymes. *Nat Chem Biol*. 2018;14(2):156-162. doi:10.1038/nchembio.2539

129. Voet D, Voet JG. *Biochemistry*. 4th ed. Hoboken, NJ: Wiley; 2010.

130. Deng C, Chen RR. A pH-sensitive assay for galactosyltransferase. *Anal Biochem*. 2004;330(2):219-226. doi:10.1016/j.ab.2004.03.014

131. Czaplinski A. Forced vital capacity (FVC) as an indicator of survival and disease progression in an ALS clinic population. *J Neurol Neurosurg Psychiatry*. 2005;77(3):390-392. doi:10.1136/jnnp.2005.072660

7. Appendices

Appendix 7.1- Acceptors tested in assays with each structure, and structure from Consortium for Functional Glycomics (CFG), the respective Molecular Mass calculated with GlycanMass tool from Expasy, and the several concentrations used in the reaction mixtures.

Name	Structure	Structures (CFG)	Molecular Mass	Concentration
Glucose	Glc		180	[5,10,20] mM
Galactose	Gal		180	20 mM
N-acetylglucosamine	GlcNAc		221	[5,10,15,20] mM
N-acetylgalactosamine	GalNAc		221	20 mM
Mannose	Man		180	20 mM
N-acetyllactosamine (LacNAc)	Galβ1-4GlcNAc		383	4 mM
Lewis^{c}	Galβ1-3GlcNAc		383	0.7 mM
Diacetylchitobiose	GlcNAcβ1-4GlcNAc		424	2 mM
Lewis^{a}	Galβ1-3(Fucα1-4)GlcNAc		529	-
Lewis^{x}	Galβ1-4(Fucα1-3)GlcNAc		529	4 mM
Lacto-N-tetraose (LNT)	Galβ1-3GlcNAcβ1-3Galβ1-4Glc	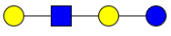	707	0.7 mM

Lacto-N-neotetraose (LNnT)	Galβ1-4GlcNAcβ1-3Galβ1-4Glc		707	0.7 mM
Lacto-N-fucopentaose I (LNFP I)	Fucα1-2Galβ-1-3GlcNAcβ1-3Galβ1-4Glc	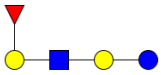	853	0.7 mM
Lacto-N-fucopentaose II (LNFP II)	Galβ1-3(Fucα1-4) GlcNAcβ1-3Galβ1-4Glc	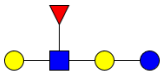	853	2 mM
Diantennary minus two Gal plus 1 bisecting GlcNAc plus proximal Fuc	FA2B	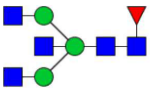	1666	10 µM
Diantennary minus two Gal plus proximal Fuc	FA2	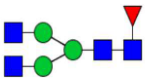	1463	10 µM
Diantennary minus two Gal	A2	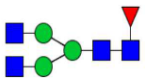	1316	10 µM
Diantennary plus bisecting GlcNAc plus proximal Fuc	FA2BG2	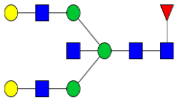	1990	10 µM
Diantennary minus one Gal plus bisecting GlcNAc plus proximal Fuc	FA2B[6]G1	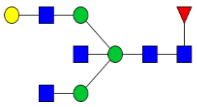	1828	10 µM
Diantennary minus two Gal plus bisecting GlcNAc	A2B	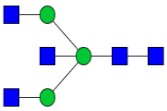	1520	10 µM
Diantennary minus one Gal plus proximal Fuc	FA2G	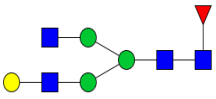	1625	10 µM
Diantennary minus one Gal	A2G	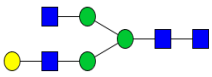	1479	10 µM
Diantennary minus two Gal minus one GlcNAc with proximal Fuc	GnM3F	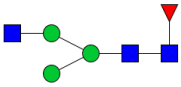	1259	10 µM
Diantennary minus two Gal minus one GlcNAc without proximal Fuc	GnM3	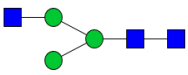	1113	10 µM

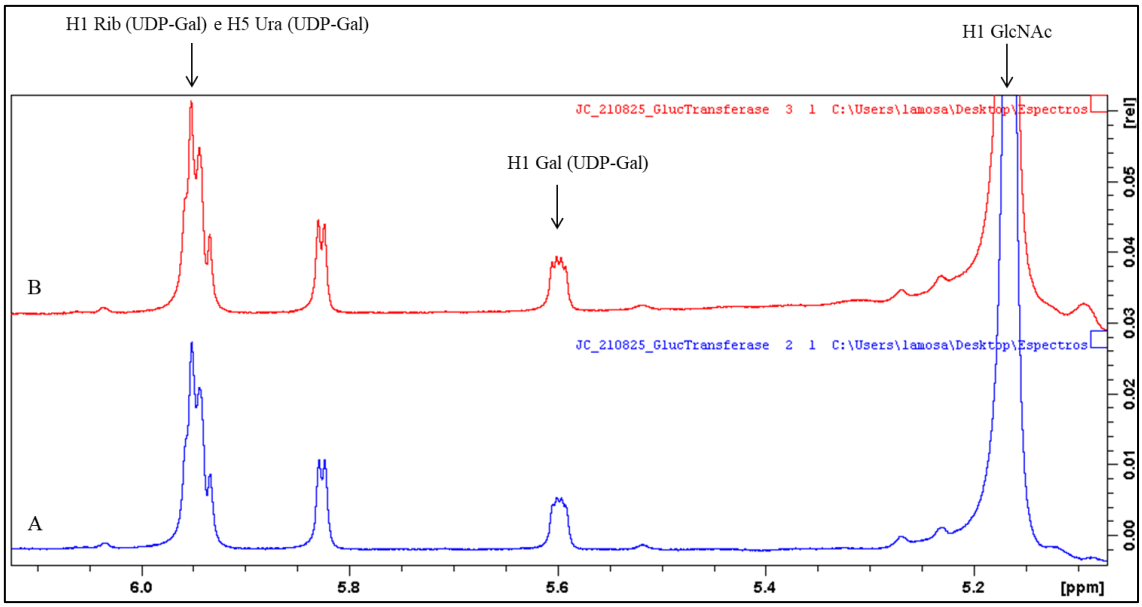

Appendix 7.2- NMR analysis of anomeric region of reaction mixture with 50 mM Tris HCl pH 7.5, 5 mM MnCl2, 5 mM UDP-Gal, 0.1 M GlcNAc, and 6.7 µL GLT8D1 in a 24 h at 37 °C incubation. Following 0.5 M EDTA. Top red spectrum **(B)** corresponds to control analysis without GLT8D1 (performed in the same conditions) whereas the bottom blue **(A)** represents the described reaction mixture. Relevant peaks are identified with the respective compounds and no differences between the spectrums were observed. Results were obtained at CERMAX (Dr. Pedro Lamosa).